To the Graduate Council:

I am submitting herewith a thesis written by Angela Whisnant entitled "Studies of Reversible Inhibition, Irreversible Inhibition and Activation of Alkaline Phosphatase by Capillary Electrophoresis". I have examined the final paper copy of this thesis for form and content and recommend that it be accepted in partial fulfillment of the requirements for the degree of the Master of Science, with a major in chemistry.

S. Douglass Gilman, Major Professor

We have read this thesis and
recommend its acceptance:

Acceptance for the Council:

Vice Chancellor and Dean of
Graduate Studies

Studies of Reversible Inhibition, Irreversible Inhibition and Activation of Alkaline Phosphatase by Capillary Electrophoresis

A Thesis presented for the Master of Science Degree

The University of Tennessee, Knoxville

Angela Randall Whisnant

May 2004

Acknowledgments

I wish to thank all those who supported me while I worked on this degree. I must first thank my husband, Jody, who supports me in whatever I choose to pursue. I also thank my little girl, Caitlin, for being the sunshine of my day and cheering me up when I so very often have needed it. I also thank my father, mother, and sister for the love and support they give me. I also thank Dr. Gilman for the ideas, guidance and encouragement that he gave me to get this project started from the very beginning to the point of being successful. I also must thank my fellow group members, especially Jason Pittman, for ideas and help given when needed. I also thank Carol Moulton for her encouragement and friendship over the years that we worked together; she will be greatly missed.

Abstract

Reversible inhibition, irreversible inhibition, and activation of calf intestinal alkaline phosphatase (EC 3.1.3.1) have been studied by capillary electrophoresis. The capillary electrophoretic enzyme-inhibitor assays were performed by electrophoretically mixing zones of inhibitor and enzyme in a substrate-filled capillary. Enzyme inhibition was indicated by a decrease in product formation detected in the capillary by laser-induced fluorescence. Reversible enzyme inhibitors could be quantified by Michaelis–Menten treatment of the electrophoretic data. Reversible, competitive inhibition of alkaline phosphatase by sodium vanadate and sodium arsenate has been examined. The calculated K_i value for the capillary electrophoretic enzyme-inhibitor assays was 2.1 μM for sodium vanadate and 21 μM for sodium arsenate. The limit of detection for sodium vanadate was 3 μM, and the limit of detection for sodium arsenate was 10 μM. Reversible, non-competitive inhibition of alkaline phosphatase by theophylline has been studied. The calculated K_i value for the capillary electrophoretic enzyme-inhibitor assays for theophylline was 102 μM, and the limit of detection was 3 μM. Irreversible inhibition of alkaline phosphatase by EDTA at concentrations of 1.0 mM or higher has been observed. Activation of alkaline phosphatase has also been observed for EDTA at concentrations from 20 to 400 μM.

Table of Contents

List of Figures

Chapter 1

Chapter 2

Chapter 3

Appendix

Nomenclature

cm	centimeter
°C	degrees Celsius
Hz	hertz
kV	kilovolt
μA	milliampere
μL	microliter
μm	micrometer
μM	micromolar
mm	millimeter
mM	millimolar
min	minute
nm	nanometer
nM	nanomolar
s	second
V/cm	volts per centimeter

Abbreviations

ADH	alcohol dehydrogenase
AttoPhos	[2,2'-bibenzothiazol]-6-hydroxy-benzathiazole phosphate
CE	capillary electrophoresis
CE-LIF	capillary electrophoresis with laser-induced fluorescence

DEA	diethanolamine
d[P]/dt	change in product concentration over time
EDTA	ethylenediaminetetraacetic acid
EGTA	ethlyene glycol-bis(2-aminoethyl)-*N*,*N*,*N*′,*N*′-tetraacetic acid
EMMA	electrophoretically mediated microanalysis
[ES]	concentration of enzyme–substrate complex
ES	enzyme–substrate complex
i.d.	inner diameter
K_i	dissociation–constant of the enzyme-inhibitor complex
K_m	Michaelis–Menten constant
K_m^*	Apparent Michaelis–Menten constant
LIF	laser-induced fluorescence
N_2	nitrogen gas
NAD^+	nicotinamide adenine dinucleotide
NADH	nicotinamide adenine dinucleotide, reduced form
NTA	nitriloacetic acid
o.d.	outer diameter
PMT	photomulitiplier tube
RI_{ce}	inhibitor response factor for CE experiments
RI_{mp}	inhibitor response factor for microplate experiments
[S]	substrate concentration
v	reaction velocity
V_{max}	maximum velocity of an enzyme reacting with substrate

V_{max}^{*}	apparent V_{max}
Zn^{+2}	zinc with +2 charge

Chapter 1

Introduction to Enzyme Assays

1.1 Enzyme Assays

Enzymes are large proteins that are found in biological systems and catalyze a wide variety of chemical reactions (1). Enzymes have an affinity for specific substrates, and the chemical structure of the substrate as well as its concentration will affect enzyme-catalyzed reaction rate of the substrate to form product (1). The substrate binds to the enzyme at a specific place called the active site. The active site is where the substrate is converted to product (2). The enzyme-catalyzed reaction may also depend on a cofactor, small inorganic ions (i.e. Mg^{+2} and Zn^{+2}), or a coenzyme, an organic molecule (i.e. NAD^{+}, nicotinamide adenine dinucleotide). The cofactors or coenzymes are bound tightly to the enzyme at a particular site on the protein molecule. The enzyme-catalyzed reaction rate also depends on other factors such as temperature, buffer composition, solvent, pH, and enzyme stability (3).

Figure 1.1 shows the general reaction scheme for an enzyme-catalyzed reaction. The velocity (v) of the reaction of substrate can be determined by plotting the concentration of product formed versus time. The rate of the reaction is as follows:

$$v = d[P] / dt = k_2 [ES] \qquad (1a)$$

Reaction of enzyme with substrate

$$E + S \underset{k_{-1}}{\overset{k_1}{\rightleftharpoons}} ES \underset{k_{-2}}{\overset{k_2}{\rightleftharpoons}} E + P$$

Production formation versus time

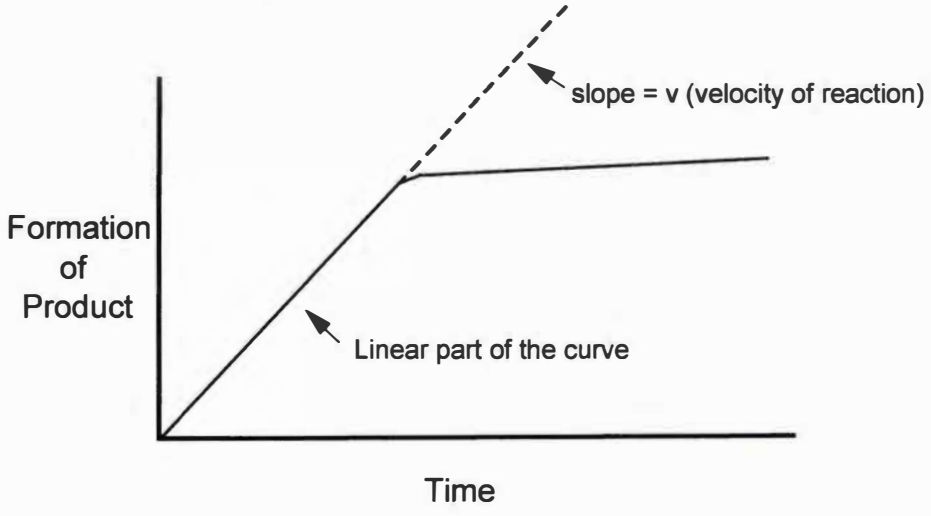

Lineweaver-Burk Plot

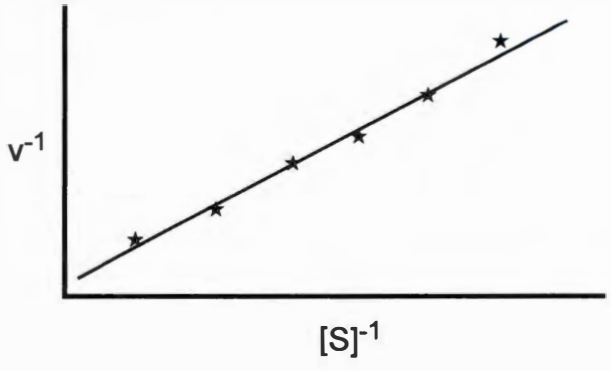

Figure 1.1. General enzyme-catalyzed reaction scheme

where d[P]/dt is formation of product over time, k_2 is the rate constant for the formation of product, and [ES] is the concentration of enzyme–substrate complex. Figure 1.1 shows the formation of product over time. Since only the initial rate of the reaction once steady state is reached is considered, the reaction where product (P) and the enzyme (E) form ES can be ignored (involving the rate constant k_{-2}) due to the small concentration of P initially (1). The reaction velocity is defined by the second step of the reaction in Figure 1.1 because it is the slowest step. The maximum velocity for the enzyme-catalyzed reaction is reached when all the enzyme is in the form of the enzyme–substrate complex. When the concentration of the enzyme-substrate complex is essentially constant because the rate of formation and disappearance of the enzyme–substrate complex is basically the same, this is then considered steady state. The reaction kinetics of the enzyme-catalyzed reactions in steady-state can be described by the following equation:

$$v = (V_{max}\ [S]) / (K_m + [S]) \qquad (1b)$$

where V_{max} is the maximum velocity of the reaction with an enzyme and a specific substrate, [S] is the concentration of substrate, K_m is the Michaelis–Menten constant, and v is the reaction velocity (1, 2). This equation is known as the Michaelis-Menten equation and be can be rearranged as follows:

$$1 / v = 1 / V_{max} + (K_m / V_{max}) / [S] \qquad (1c)$$

Equation 1c is called the Lineweaver–Burk equation, and a plot of v^{-1} versus $[S]^{-1}$ is called a Lineweaver–Burk plot or double-reciprocal plot (2). Measuring the rate of the reaction, v, at different substrate concentrations and plotting the data using

the Lineweaver–Burk equation will allow the determination of V_{max} from the *y*-intercept and K_m from the slope of the line. Figure 1.1 shows an example of a Lineweaver–Burk plot.

The rate of the enzyme-catalyzed reaction can be monitored by measuring either product formation or disappearance of substrate using several detection methods such as absorbance (4), fluorescence (4), and electrochemical detection (5–7). The reaction can be initiated by either adding the enzyme to a mixture containing all required chemicals such as the substrate, buffer, enzyme, cofactors, or coenzyme and monitoring the reaction or adding the substrate to a mixture with the required chemicals (3). The initial rate of the reaction, v, is determined from the initial, linear part of the curve (Figure 1.1) of a plot of product concentration versus time or substrate concentration versus time (3). For example, alcohol dehydrogenase (ADH) reacts with ethanol to form acetaldehyde (8). Alcohol dehydrogenase requires the coenzyme NAD^+ in order to catalyze the reaction of ethanol to actealdehyde. During the reaction, NAD^+ is converted to NADH (nicotinamide adenine dinucleotide, reduced form). The reaction is as follows:

$$CH_3CH_2OH + NAD^+ \overset{ADH}{\longleftrightarrow} CH_3CHO + NADH + H^+ \qquad (1d)$$

To determine the kinetic factors (V_{max} and K_m) for the reaction of ethanol with ADH, a traditional experiment would be as follows. Ethanol and NAD^+ would be added to a cuvette. The cuvette would then be placed in a UV/VIS spectrometer. Then the ADH is added to the cuvette, and the concentration of NADH is

monitored by absorbance at 340 nm. The plot of NADH concentration versus time would be similar to the plot in Figure 1.1. The slope of the initial, linear part of the curve would be used to determine v at the specific concentration of the substrate, ethanol (with NAD^+ in excess). The same experiment would be performed at several concentrations of ethanol as the limiting reagent in order to construct a Lineweaver–Burk plot (Figure 1.1) to determine V_{max} and K_m for the ADH-catalyzed reaction of ethanol. Such experiments can be performed at a smaller scale and in parallel using microwell plates (e.g. 96; 384 wells/plate), but the experiments are effectively identical to a series of experiments performed in a standard cuvette.

1.2 Enzyme Inhibition

Enzymes catalyze the reaction of a specific substrate. Enzyme inhibition occurs when another substance interferes in the enzyme-catalyzed reaction. The inhibitor will cause the rate of reaction to decrease. The inhibitor may also inactivate the enzyme completely (1).

Enzyme inhibition is important in many scientific areas including pesticide science and pharmacology. Enzyme inhibitors are developed as pesticides to protect crops from damage caused by insects (9, 10). Compounds are designed to inhibit specific enzymes for medical applications (11, 12). For example, metal complexes developed to inhibit enzymes are used as drugs to treat cancer, hypertension, and arthritis (13). Many chemical analysis methods have been developed using enzyme inhibition reactions. Environmental pollutants,

organophosphorus pesticides, and heavy metal ions have all been studied through inhibition of reactions catalyzed by various enzymes (14).

There are two types of inhibition: reversible and irreversible (1). In reversible inhibition, once the inhibitor is removed, the enzyme activity will return to its previous level. There are several different types of reversible inhibitors—competitive, noncompetitive, and uncompetitive (1). Figure 1.2 presents the reaction pathways the different types of reversible inhibitors can follow (2). In Figure 1.2, K_i is the dissociation-constant of the enzyme–inhibitor complex and indicates how strong an inhibitor is for a particular enzyme.

A competitive inhibitor binds to the active site and will only bind to the free enzyme. A competitive inhibitor will also likely resemble the substrate structurally (1). The following equation based on the Michaelis–Menten equation describes the kinetics for a competitive inhibitor (15):

$$v_{i,c} = \{V_{max}\,[S]\} / \{K_m\,(1 + [I] \bullet K_{i,c}^{-1}) + [S]\} \qquad (1e)$$

When Equation 1e is rearranged into the form of the Lineweaver–Burk equation, and $1/v$ versus 1/[S] is plotted at different concentrations of inhibitor, it is determined that the V_{max} will not change, but the K_m will change as a function of [I]. The V_{max} stays the same because at high enough concentrations of substrate the effect of the inhibitor will disappear, but the K_m value is affected. From the slope of the Lineweaver–Burk plot for a competitive inhibitor, the K_m value appears as an apparent K_m^* as described by the following equation:

$$K_m^* = K_m\,(1 + [I] \bullet K_{i,c}^{-1}) \qquad (1f)$$

Competitive Inhibition

Noncompetitive Inhibition

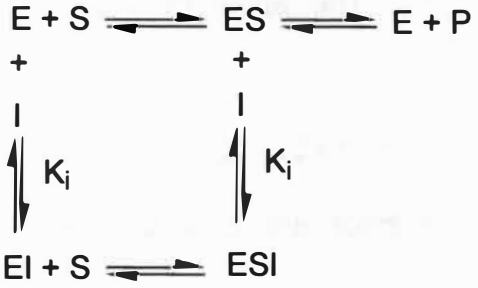

Uncompetitive Inhibition

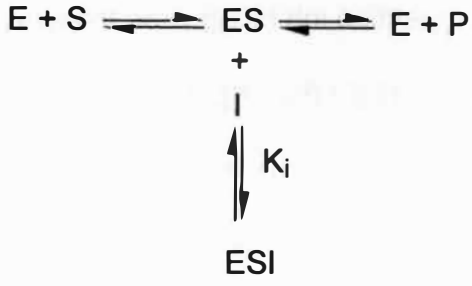

Figure 1.2. Reaction pathways for reversible inhibitors

A noncompetitive inhibitor does not bind to the active site but somewhere else on the enzyme. The noncompetitive inhibitor can bind with either the enzyme or the enzyme–substrate complex (1). The following equation describes the kinetics of a noncompetitive inhibitor (15):

$$v_{i,nc} = \{V_{max}\,[S]\} / \{K_m\,(1 + [I] \bullet K_{i,nc}^{-1}) + [S]\,(1 + [I] \bullet K_{i,nc}^{-1})\} \qquad (1g)$$

If Equation 1g is rearranged in the form of a Lineweaver–Burk plot and $1/v$ versus $1/[S]$ is plotted at different concentrations of inhibitor, it is determined that the K_m will not change but the V_{max} will. This because the inhibitor will prevent some fraction of enzyme from being able to catalyze the reaction of substrate to form product without affecting K_m. The apparent V_{max}^* can be described by the following equation:

$$1 / V_{max}^* = (1 / V_{max}\,K_i)\,[I] + 1 / V_{max} \qquad (1h)$$

An uncompetitive inhibitor will only bind with the enzyme–substrate complex. Inhibition caused by uncompetitive inhibitors with a single substrate is rare, but is seen more often in reactions with multiple substrates (1). The equation to describe uncompetitive inhibition is as follows:

$$v_{i,uc} = \{V_{max}\,[S]\} / \{K_m + [S]\,(1 + [I] \bullet K_{i,uc}^{-1})\} \qquad (1i)$$

from rearrangement of Equation 1i in the form of the Lineweaver–Burk plot of $1/v$ versus $1/[S]$ and plotting at different inhibitor concentrations, it is determined that V_{max} and K_m are both affected by an uncompetitive inhibitor (15).

In irreversible inhibition, once the inhibitor is removed, the enzyme activity will not increase (1). Many irreversible inhibitors can form a covalent bond with a particular functional group of an amino acid in the protein structure of the

enzyme, and thus change the enzyme conformation or affect the active site geometry and cause the enzyme activity decrease. Some enzymes contain cofactors and can be irreversibly inhibited by using a metal chelator to remove the cofactor from the enzyme. The initial enzyme activity will only return if the metal cofactor is added back to the enzyme. If the cofactors or coenzymes are removed and not to bound the enzyme, the enzyme is inactivated and is called an apoenzyme. Irreversible inhibitors have been used as tools to learn more about enzyme active sites and enzyme mechanisms (1). The detailed kinetics of irreversible inhibitors are more complex and difficult to study compared to reversible inhibitors. Often the percentage of the activity of the enzyme remaining versus time at different concentrations of inhibitor can show how strong the irreversible inhibition is (16–19). Also the rate constants for irreversible inhibition can be determined by a complex method called the Tsou method (18, 19).

1.3 On-line Enzyme Assays

Capillary electrophoresis has emerged as a versatile tool for enzyme analysis (20, 21). Homogeneous on-column capillary electrophoretic enzyme assays, where the enzyme is injected into the capillary as a discrete zone, offer several advantages. These include simplicity, rapid analysis times, minimal sample preparation, and consumption of extremely small amounts of enzyme (20, 21). Single enzyme molecules have been detected and studied (22, 23), and separation and detection of isoenzymes from single cells have been reported (24). Either the substrate or enzyme concentration can be quantified (8, 20, 25,

26), and Michaelis–Menten constants can be determined (27–31). Peptide mapping using on-column enzyme digestion has also been demonstrated (32), and enzymatic digestion of oligonucleotides has been studied (33).

The first on-column capillary electrophoretic enzyme assays, which described by Bao and Regnier (25), were performed by injecting a zone of enzyme into a capillary filled with substrate and the required coenzyme for the catalyzed reaction. Product was formed as the enzyme migrated through the capillary, and the product was detected at a downstream absorbance detector. This type of assay, based on a reaction carried out in a CE column, was later termed electrophoretically mediated microanalysis (EMMA), and this specific format was defined as "continuous-engagement" EMMA (34, 35). Capillary electrophoretic enzyme assays have also been carried out by injecting the enzyme and substrate as two separate zones and allowing the zones to mix electrophoretically (36). Product was formed when the enzyme and substrate zones mixed electrophoretically, and this product was detected as a separate zone. This format was defined as "transient-engagement" EMMA (34, 35). Figure 1.3 illustrates both types of EMMA.

Enzyme assays based on EMMA have been used to quantify enzyme and substrate, to determine Michaelis–Menten constants, and to determine enzyme activity (20, 21, 25, 30) (34, 35, 37–43). Enzyme assays have been developed using microchip devices (44). Many of these enzyme assays on microchip devices utilize electrophoretic mixing of reagents (EMMA) (28, 44–47). Capillary

"Continuous-engagement" EMMA

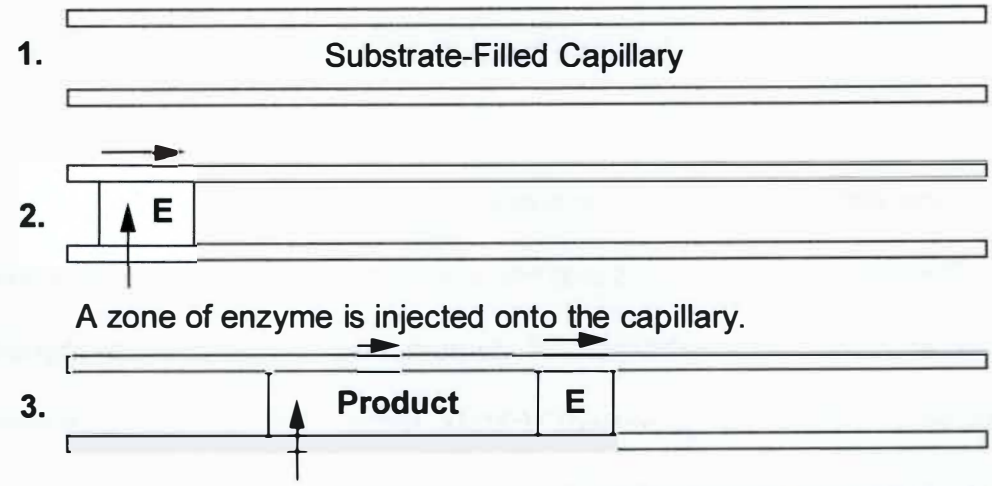

Product forms as enzyme migrates through the substrate-filled capillary.

"Transient-engagement" EMMA

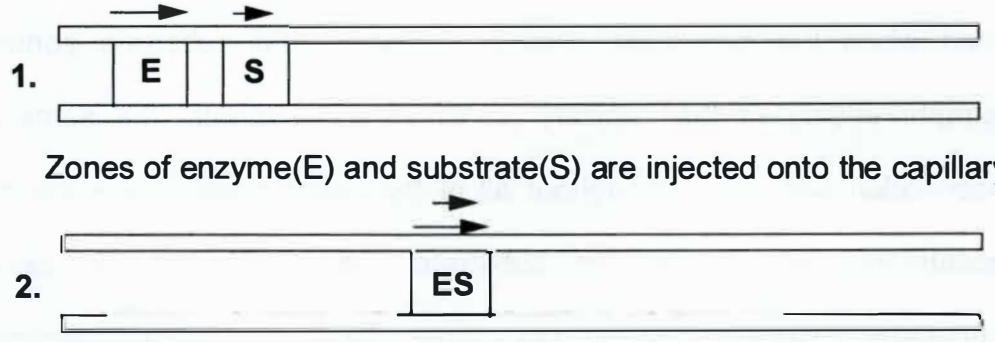

The enzyme and substrate mix electrophoretically and will form product(P).

The zones will electrophoretically separate and be detected.

Figure 1.3. Description of the two types of EMMA

electrophoresis and electrophoretic microchip devices have also been used to study enzyme reactions by incubating reagents together, injecting an aliquot of the reaction mixture into a capillary or onto a microchip, and separating and detecting product formed during the incubation prior to injection (20, 21, 48-53).

1.4 On-line Enzyme-Inhibition Assays

Capillary electrophoresis and electrophoretic microchip devices have been used to study enzyme inhibition. A combination of "continuous-engagement" EMMA and "transient-engagement" EMMA techniques has been developed to study enzyme inhibition by CE (54). In these experiments, the running buffer contained *erythro*-9-(2-hydroxy-3-nonyl)adenine, a competitive inhibitor of adenosine deaminase. The substrate was adenosine. The product, inosine, was formed when the individually injected enzyme and substrate zones mixed electrophoretically in the capillary. In these experiments, the same inhibitor concentration was used throughout all of the experiments, while the substrate concentration was varied. The substrate and the enzyme solutions were preincubated independently with the inhibitor for 10 min before injection. When the injected enzyme and substrate zones had mixed electrophoretically in the capillary, the enzyme was allowed to incubate with the substrate at zero potential for 5 min. The high voltage was applied again, and the product was separated and detected by absorbance at 254 nm. Lineweaver–Burk plots for the data were used to determine the K_i for *erythro*-9-(2-hydroxy-3-nonyl)adenine.

"Transient-engagement" EMMA method was used to study the inhibition of rhodanese by 2-oxoglutarate (55). The enzyme-catalyzed reaction requires two substrates, thiosulfate and cyanide. In the reaction, a sulfur from the thiosulfate ion is transferred to the cyanide ion to form the product, thiocyanate. The CE experiment is performed by injecting a zone of the enzyme and a separate zone containing the substrates and inhibitors, which are preincubated together before injection. Bromide was also used as an internal standard. The product, thiocyanate, was detected by UV/VIS absorbance. The K_i values for the inhibitor as well as the type of inhibition with respect to each of the substrates were determined for each inhibitor.

Enzyme inhibition has also been studied using electrophoretic mixing in microchip devices (27–29). The first report of this type of assay using continuous-engagement EMMA was for the enzyme, β-galactosidase (28). The fluorogenic substrate, resorufin β-d-galactopyranoside, was used, and the competitive inhibitor, phenylethyl β-d-thiogalactoside, was studied. Substrate, buffer, enzyme, and inhibitor were contained in separate reservoirs on the microchip device and were mixed in the device by electrokinetic transport controlled by applied potentials. The substrate concentration was controlled by mixing substrate and buffer in the device under potential control. Enzyme and inhibitor solutions at fixed concentrations were subsequently mixed with the diluted substrate solution, and product formation was detected in the final reaction channel at a

downstream LIF detector. The K_i was determined for phenylethyl β-d-thiogalactoside, and inhibition by two additional inhibitors was detected.

A related microchip assay was developed for observing protein kinase A inhibition by H-89, a known competitive protein kinase A inhibitor (27). The substrate was fluorescently labeled Kemptide, a heptapeptide that is not fluorogenic. In these experiments, the inhibitor was diluted on the microchip device and mixed with fixed concentrations of enzyme and substrate. Aliquots of the sample stream containing enzyme, substrate, and inhibitor were injected on the microchip device by into a separation channel after 75 seconds of incubation in an incubation channel. Then, the product and substrate were separated electrophoretically and detected by fluorescence. The K_i value for the inhibitor was determined.

A microchip assay was applied to study inhibition of acetylcholinesterase using acetylthiocholine as a substrate (29). Competitive and irreversible acetylcholinesterase inhibitors were examined using continuous-engagement EMMA. The enzyme was continuously pumped through the microchip device. Substrate was added to the enzyme stream. The product of the enzyme reaction is not fluorescent; therefore, coumarinylphenylmaleimide was added on-column after product formation to derivatize the product for LIF detection. Discrete zones of inhibitor were injected into the enzyme stream before the point of substrate addition, and inhibition was indicated by a decrease in fluorescent product formation as the inhibitor zone migrated to the detector. The K_i was determined for the competitive inhibitor, tacrine. Using this method, reversible and

irreversible inhibitors could be analyzed and distinguished. Separation and detection of a mixture of inhibitors was demonstrated.

Presented here, different classes of alkaline phosphatase inhibitors have been investigated by CE using a combination of continuous-engagement EMMA and transient-engagement EMMA. These inhibitors include a non-competitive, reversible inhibitor (theophylline), competitive, reversible inhibitors (sodium vanadate and sodium arsenate) and an irreversible inhibitor (EDTA). Theophylline, sodium vanadate, and sodium arsenate were quantified, and their K_i values were determined. The activity change of the enzyme was quantified for experiments with EDTA. The specific enzyme studied was alkaline phosphatase (EC 3.1.3.1 from calf intestine).

Chapter 2

Capillary Electrophoretic Analysis of Alkaline Phosphatase Inhibition by Theophylline

2.1 Introduction

An on-column capillary electrophoretic enzyme-inhibition assay with fluorescence detection was developed to study the inhibition of alkaline phosphatase by theophylline. Theophylline is a non-competitive, reversible inhibitor of alkaline phosphatase (56). Reported K_i values for theophylline with alkaline phosphatase range from 78 μM for bovine liver alkaline phosphatase to 135 μM for serum alkaline phosphatase (57, 58). Theophylline is a clinically important compound that is used as a bronchodilator, respiratory stimulant, anti-inflammatory drug, and for apnea treatment (59–61). The inhibition of alkaline phosphatase by theophylline is a good model system for developing these online enzyme–inhibitor assays because theophylline inhibition of alkaline phosphatase has been studied extensively, and it is potent inhibitor of this enzyme. Its reversible behavior would be easily observed in the electropherogram.

Described here is the initial development of the on-column capillary electrophoretic enzyme-inhibition assay using the inhibition of alkaline phosphatase by theophylline. In the enzyme-inhibition assay presented in this chapter, the capillary is filled with a fluorogenic substrate. Next, separate zones

of the inhibitor and enzyme are injected. As the zones of the inhibitor and enzyme migrate through the capillary at a constant applied potential, product is continuously formed. When the zones of inhibitor and enzyme mix, the product formation decreases. When the zones of inhibitor and enzyme disengage, the product formation returns to its previous level.

2.2 Experimental

2.2.1 Reagents

Alkaline phosphatase (EC 3.1.3.1 from calf intestine) was purchased from ICN Biomedicals (Aurora, OH). AttoPhos ([2,2'-bibenzothiazol]-6-hydroxy-benzathiazole phosphate) was obtained from Promega (Madison, WI). Theophylline (99%) and diethanolamine (DEA) were supplied by Acros (Pittsburgh, PA). All solutions and buffers were prepared in ultrapure water (>18 MΩ•cm, Barnstead E-pure System, Dubuque, IA).

2.2.2 CE-LIF Instrumentation and Experimental Conditions

The capillary electrophoresis instrument with laser-induced fluorescence detection (CE-LIF) was constructed in-house. The 457.9 nm line of a Coherent INNOVA 90C-5 argon ion laser (Santa Clara, CA) was used for excitation. The laser beam was focused onto the capillary by a fused-silica plano convex lens (f = 15.0 mm) (Optosigma, Santa Ana, CA). The power of the laser beam at the capillary was 35 mW. The fluorescence was collected at 90° to the laser beam by

a 20X microscope objective (Edmund, Barrington, NJ) and was filtered by a 560 ± 10 nm bandpass filter (Oriel, Stratford, CT). A 1 mm diameter aperature (Oriel) was used as a spatial filter. Fluorescence was detected by a PMT (HC120, Hamamatsu, Bridgewater, NJ) at 750 V. The PMT output was filtered by a low-pass filter at 50 Hz, and then sent to an analog-to-digital board (Lab-PC-1200, National Instruments, Austin, TX). A LabVIEW program (National Instruments) was written in-house for data acquisition. The sampling rate was 10 Hz. The data were analyzed using Excel (Microsoft) and Peakfit (SPSS Inc., Chicago, IL). A Spellman high-voltage power supply (CZE1000R, Hauppauge, NY) was used for the electrophoresis system. Fused silica capillaries with a 50 μm i.d. and 220 μm o.d. (SGE, Austin, TX) were utilized. The detection window was made by burning away the polyimide coating.

The running buffer contained 50 mM DEA at pH 9.5 and 0.10 mM AttoPhos, a fluorogenic alkaline phosphatase substrate. The enzyme solution contained 0.18 nM alkaline phosphatase and 50 mM DEA buffer at pH 9.5. The running buffer and enzyme solution were prepared fresh daily. In addition to the inhibitor, the inhibitor solutions contained 0.10 mM AttoPhos and 50 mM DEA at pH 9.5. The applied electric field was 310 V/cm for all separations and injections. All injections were performed electrokinetically. The electrode and capillary were rinsed externally with 50 mM DEA buffer at pH 9.5 before and after each injection in order to prevent cross contamination of the running buffer, enzyme solution and inhibitor solutions.

The capillary was thermostatted by enclosing the capillary from the injection end to the detection window in Teflon tubing (1.6 mm i.d.; 3.2 mm o.d.) (Nalgene, Rochester, NY) and flowing heated N_2 gas (40 °C) through the Teflon tubing around the capillary. To ensure that the air flowed evenly over the entire thermostatted section of the capillary, two pieces of Teflon tubing of equal length were placed over the capillary from the injection end to the detection window. The two pieces of Teflon tubing were connected by a T-union Swagelock fitting. The third connection to the T-union was the tubing from the heated N_2 source. The end of the tubing at the injection end of the capillary and at the detection window were sealed with Duco cement. To allow air flow, two small holes were placed in the Teflon tubing at equal distances from the injection end and the detection window. This reduced evaporation of solution in the buffer reservoirs by directing N_2 flow away from the reservoirs. At the injection end, 1 cm of the capillary was not enclosed in Teflon tubing.

2.2.3 Microplate Experiments

Experiments were performed using a FLUOstar microplate fluorometer (BMG, Durham, NC). The excitation filter was centered at 450 nm, and the emission filter was centered at 555 nm. The instrument was thermostatted at 25 ^{o}C. Microplates used were 96-well plates from Nunc (V-96 Polypropylene MicroWell Plate, Roskilde, Denmark). For the inhibitor assays, each well contained final concentrations of 0.10 mM AttoPhos, 50 mM DEA at pH 9.5, and

the inhibitor at various concentrations. For the assays used to generate Lineweaver–Burk plots, each well contained a final concentration of 50 mM DEA at pH 9.5, and AttoPhos at various concentrations. Each well contained a final volume of 200 μL. For all enzyme assays, 10 μL of alkaline phosphatase were injected into each well separately by the instrument to give a final concentration of 0.18 nM. The product formation was measured at 0.1 s intervals.

2.3 Results and Discussion

2.3.1 On-column Capillary Electrophoretic Assay of Alkaline Phosphatase

Alkaline phosphatase has been the subject of several studies using on-column capillary electrophoretic enzyme assays. EMMA has been used to observe the catalyzed reaction between alkaline phosphatase and the substrates, *p*-aminophenylphosphate and *p*-nitrophenylphosphate (62). Michaelis–Menten constants for alkaline phosphatase have been determined using the EMMA technique (30). Catalysis by single alkaline phosphatase molecules has been studied using CE (63).

Figure 2.1 presents the results of an alkaline phosphatase enzyme assay without inhibitor. The assay in Figure 2.1 was performed by injecting a 3.0 s zone of 0.18 nM alkaline phosphatase at a potential of 17.8 kV (310 V/cm). Then a constant potential of 17.8 kV (310 V/cm) was applied, and the product formed continuously as the alkaline phosphatase–AttoPhos complex migrated through the capillary until the enzyme migrated past the detector. The buffer containing

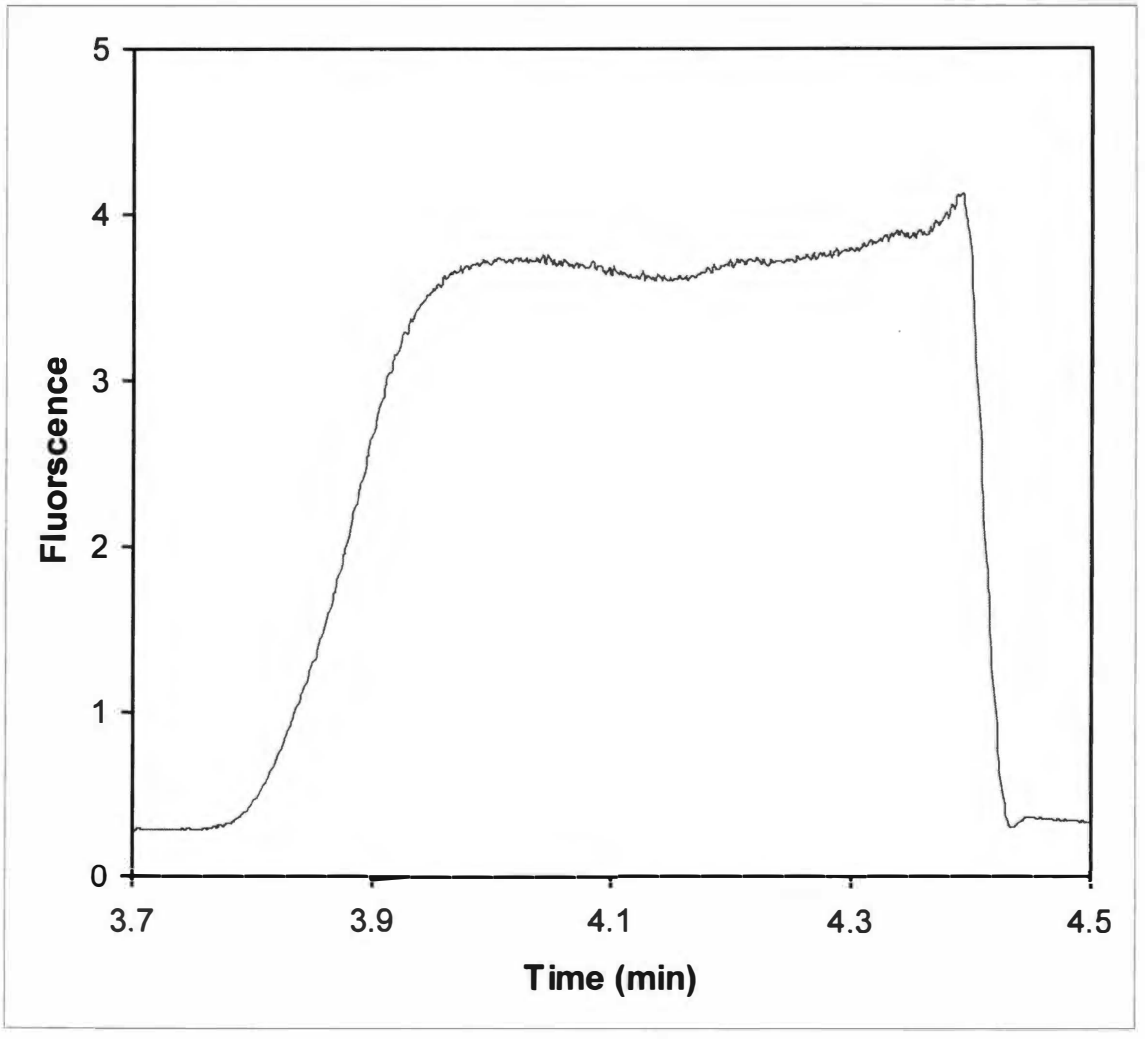

Figure 2.1. Electropherogram of an alkaline phosphatase enzyme assay with no inhibitor

diethanolamine and AttoPhos at a pH of 9.5 produced a current around 10 μA during electrophoresis.

The peak at the end of the plateau at 4.4 min (Figure 2.1) is an artifact resulting from product formation after then enzyme has been injected into the capillary and before the high voltage has been reapplied. The zero field incubation that results in this artifact is the basis of experiments designed to observe single enzyme molecules (22, 24). This artifact is observed at the end of the fluorescence plateau opposite of where one might expect it. Because the enzyme–substrate complex migrates to the LIF detector faster than the fluorescent product, the first product detected is product produced near the end of the experiment just as the enzyme–substrate complex migrates past the detector. The product produced when the enzyme is first injected into the capillary is actually detected last. In effect, all the electropherograms shown are reversed in time from what one would expect. This phenomenon has been described previously (25).

It was determined experimentally that thermostatting was important in order to maintain a constant temperature and reaction rate throughout the capillary. The capillary was enclosed in a Teflon tube and heated N_2 was circulated over the capillary in order to maintain a constant temperature. The temperature of the N_2 was optimized for maximum activity (40 °C). Figure 2.2 presents the data from an alkaline phosphatase enzyme assay without inhibitor and without thermostatting. The peaks and valleys in the electropherogram are

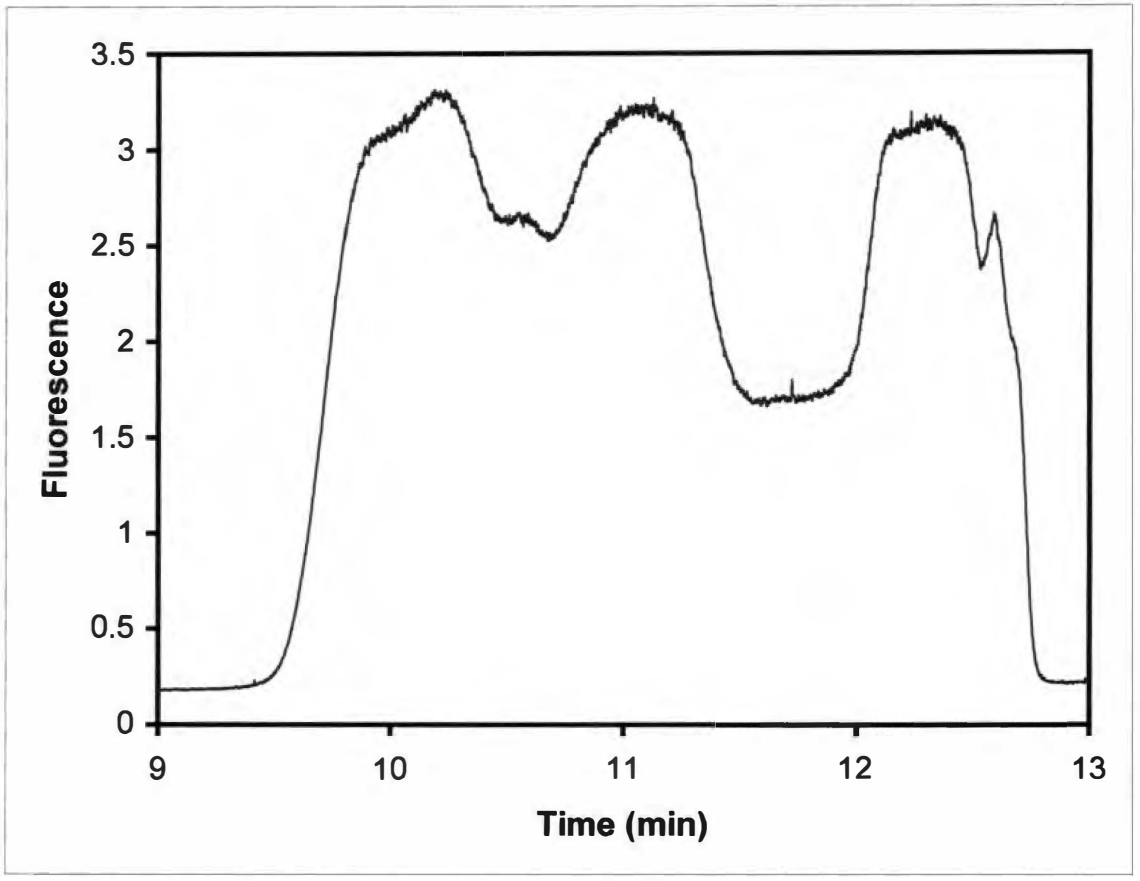

Figure 2.2. Electropherogram without thermostatting

due to changes in the temperature in different regions of the capillary which change the reaction rate as the enzyme zone passes through these regions.

2.3.2 Capillary Electrophoretic Enzyme-Inhibitor Assay of Alkaline Phosphatase

Figure 2.3 presents the data for the reversible inhibition of alkaline phosphatase by theophylline. In this experiment, 100 μM theophylline was injected first for 4.0 s at 17.8 kV (310 V/cm). Once theophylline was injected, then a constant potential of 17.8 kV was applied for 20.0 s. Next, 0.18 nM alkaline phosphatase was injected for 3.0 s at 17.8 kV, and finally the separation potential of 17.8 kV was applied. As the zones of inhibitor and enzyme–substrate complex migrated through the capillary, product was formed continuously. When the zones of inhibitor and enzyme–substrate complex mixed electrophoretically, a decrease in product formation was observed due to the inhibition of the enzyme. Once the zones of inhibitor and enzyme–substrate complex separated again, the enzyme returned to its original activity indicating that theophylline is a reversible inhibitor. The reversible inhibition of alkaline phosphatase by theophylline is readily observed in the product plateau.

Figure 2.3 (a)–(c) shows the relative positions of the enzyme and inhibitor zones in the capillary at the corresponding positions in the electropherogram. At (a), the inhibitor zone was injected first and then the enzyme zone. At (b), the two zones have electrophoretically mixed and results in

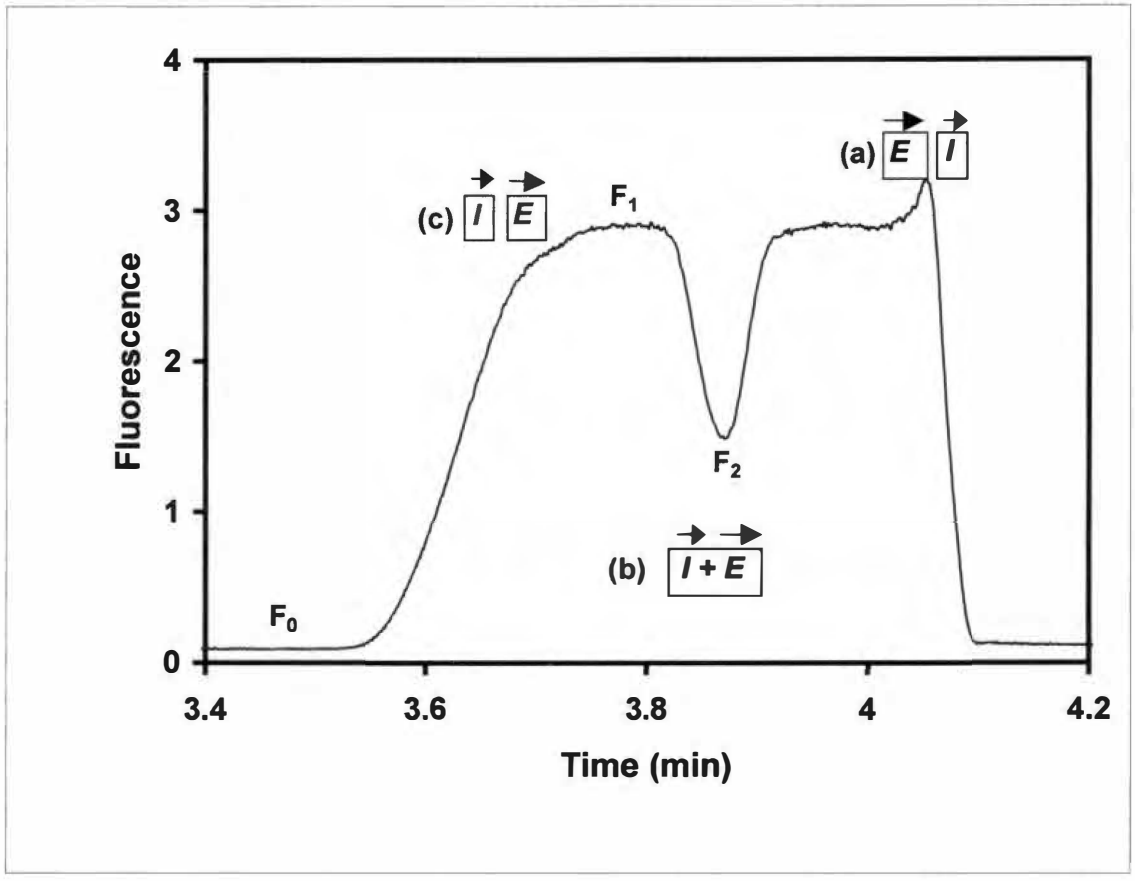

Figure 2.3. Electropherogram of an alkaline phosphatase–-theophylline enzyme–inhibition assay

the inhibition of the enzyme. At (c), the two zones separated and the activity of the enzyme returned to its initial level.

Theophylline was injected first because the enzyme–substrate complex has a greater mobility than the inhibitor. The injection order required to observe enzyme inhibition depends on the relative migration rates of the enzyme and inhibitor zones. In this case, theophylline migrates slower than the enzyme–substrate complex. Therefore, theophylline is injected first to ensure that the two zones will mix in the capillary. If the inhibitor migrates faster than the enzyme–substrate complex, the enzyme must be injected first to ensure mixing. Two experiments, at most, must be performed to detect an inhibitor of unknown electrophoretic mobility relative to the enzyme. If the inhibitor is injected first, and no inhibition is observed, a second experiment in which the enzyme is injected first should result in detection of inhibition. The exception to this would be in those rare instances where the inhibitor and enzyme have nearly identical electrophoretic mobilities.

2.3.3 Theophylline Quantitation

Theophylline is a noncompetitive, reversible inhibitor of alkaline phosphatase (56). Using Michaelis–Menten treatment of this system, the K_m value will remain the same at any inhibitor concentration, but the apparent V_{max} will change with the inhibitor concentration. The Michaelis-Menten equation is as follows:

$$v / V_{max} = [S] / (K_m + [S]) \qquad (2a)$$

where v is the initial reaction velocity, K_m is the Michaelis constant for the ES complex, and [S] is the substrate concentration (64). A relative velocity equation can be derived for a noncompetitive inhibitor (64):

$$V_{max}^{*} / V_{max} = K_i / (K_i + [I]) \quad (2b)$$

where V_{max}^{*} is the apparent V_{max} at a given inhibitor concentration, V_{max} is the maximum velocity of the enzyme in the absence of an inhibitor, K_i is the equilibrium constant for inhibitor binding to the enzyme, and [I] is the inhibitor concentration. Equation 2b can be rearranged to give the following equation:

$$1 / V_{max}^{*} = (1 / V_{max} K_i) [I] + 1 / V_{max} \quad (2c)$$

A plot of $1/V_{max}^{*}$ versus inhibitor concentration should be linear if the Michaelis–Menten treatment is appropriate.

An inhibitor response factor was defined in order to quantitate theophylline. The inhibitor response (RI_{ce}) for the capillary electrophoresis experiments is:

$$RI_{ce} = (F_1 - F_0) / (F_2 - F_0) \quad (2d)$$

The fluorescence at F_1 (Figure 2.3) is proportional to the rate of product formation without inhibitor and is used to normalize the data due to variability in the magnitude of the plateau from experiment to experiment. F_2 (Figure 2.3) is the fluorescence at the time when minimum product formation is observed, and the fluorescence is proportional to the velocity of product formation (dP/dt) during maximum inhibition. In all experiments, a saturating substrate concentration is used. Under these experimental conditions, dP/dt is V_{max}^{*}. The observed baseline signal for the experiment is F_o (Figure 2.3). Thus, RI_{ce} is proportional to $1/V_{max}^{*}$.

The RI_{ce} values at different theophylline concentrations have been plotted, and the results are shown in Figure 2.4. The K_i value was determined to be 102 ± 4 μM (R^2 = 0.997) and is in agreement with reported literature values (57, 58). The detection limit for theophylline was 3 μM, and the linear dynamic range spanned from 5 μM to 250 μM.

Similar experiments were also performed using a microplate reader. Figure 2.5 shows a plot of an analogous response factor for the microplate fluorometer, RI_{mp}, versus theophylline concentration for the microplate reader. RI_{mp} is equal to 1/slope where slope is defined from the data obtained from the microplate reader. These data were obtained by monitoring the product formation at 0.1 s intervals after the injection of alkaline phosphatase. The slope of the curve (fluorescence vs. time) was determined and is proportional to V_{max}^*. The calculated K_i for theophylline is 110 ± 5 μM (R^2 = 0.997) for the microplate enzyme-inhibitor assays. This analysis of the data assumes steady-state kinetics. The data in Figure 2.5 suggest that the CE experiments exhibit steady-state behavior.

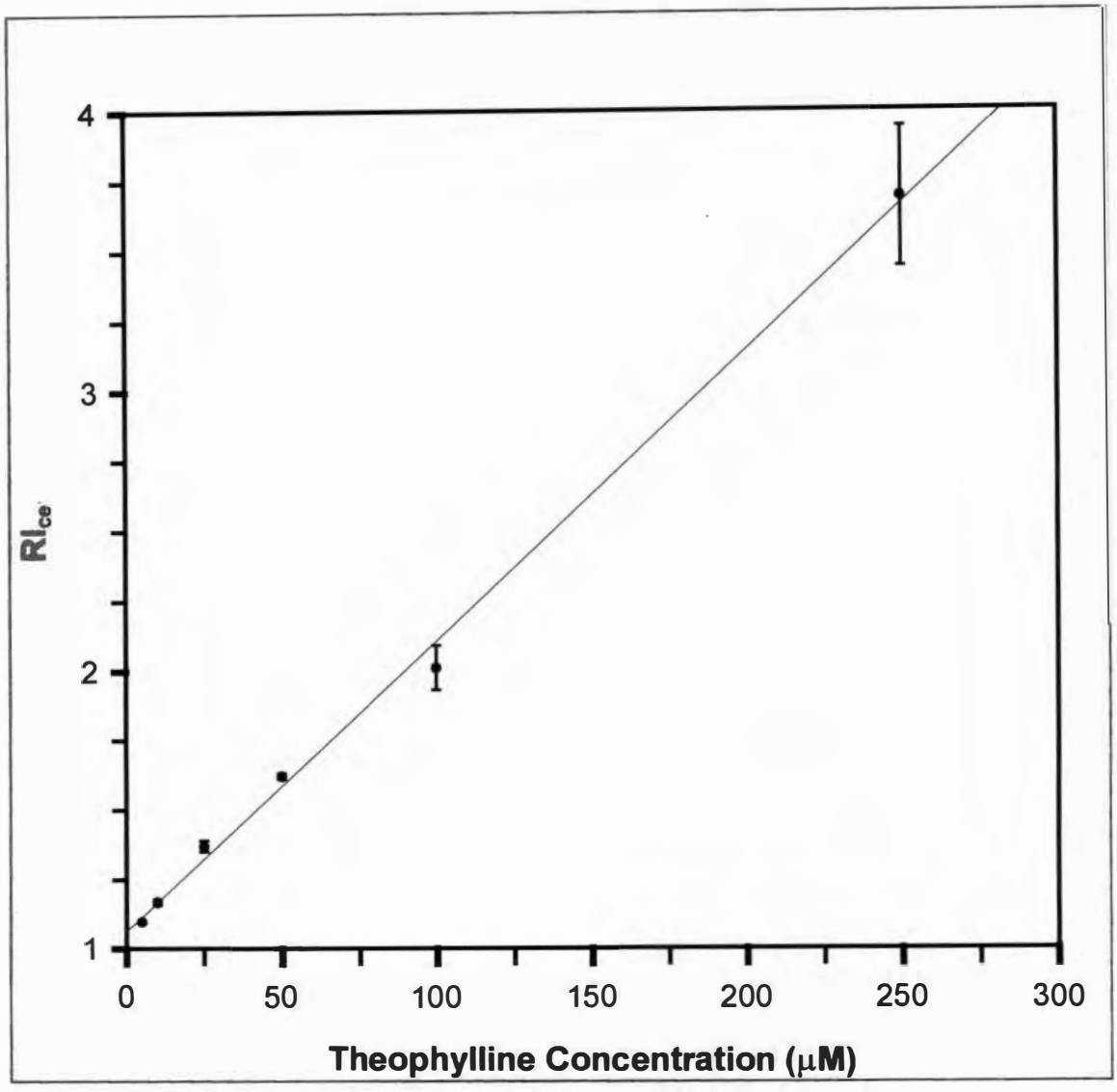

Figure 2.4. Plot of RI_{ce} versus theophylline concentration

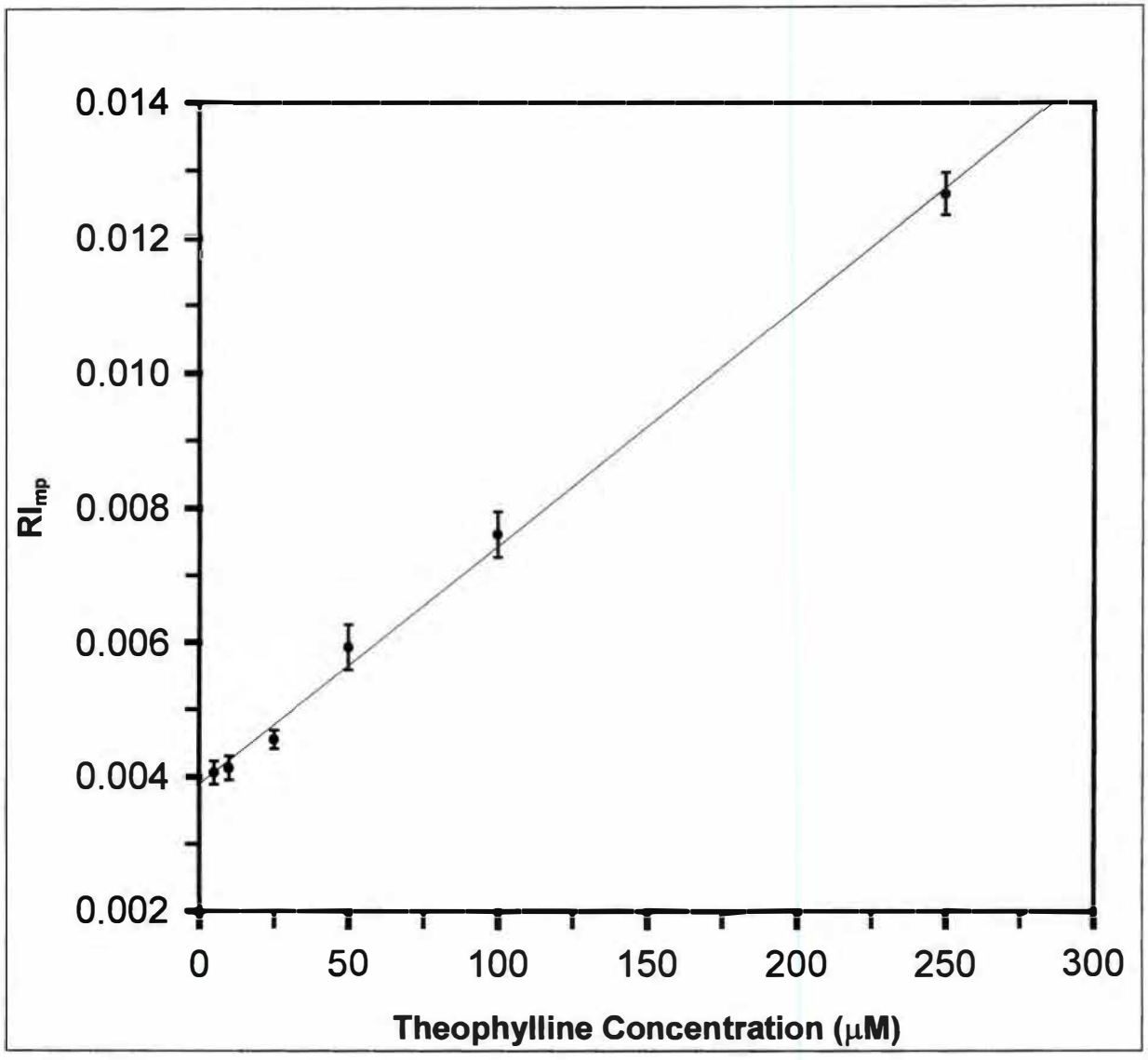

Figure 2.5. Plot of RI_{mp} versus theophylline concentration

Chapter 3

Capillary Electrophoretic Analysis of Alkaline Phosphatase Inhibition by Irreversible and Competitive, Reversible Inhibitors

3.1 Introduction

The first inhibitor of alkaline phosphatase studied was theophylline, which is a reversible, noncompetitive inhibitor of alkaline phosphatase. There are several other important classes of inhibitors, and in order to expand the utility of this technique, other classes of inhibitors were also studied. These inhibitors include competitive, reversible inhibitors, sodium vanadate and sodium arsenate, and the irreversible inhibitor, EDTA.

Sodium vanadate is a competitive, reversible inhibitor of alkaline phosphatase (56, 65–67). Reported K_i values for sodium vanadate range from 4 μM for rat intestinal alkaline phosphatase (67) to 12 μM for *Escherichia coli* alkaline phosphatase (66). Vanadate is used in the treatment of diabetes since it mimics the effects of insulin and reduces glucose levels (68–70). In the body, vanadate affects the activity of several enzymes including adenylate cyclase, which regulates the levels of cyclic adenosine monophosphate. Cyclic adenosine monophosphate affects insulin secretion (70). Sodium arsenate, also a reversible, competitive inhibitor of alkaline phosphatase, was studied (56, 65, 67, 71). Reported K_i values for sodium arsenate range from 2 μM for rat intestinal

alkaline phosphatase (67) to 33.8 μM for membrane-bound alkaline phosphatase from bone cartilage (65).

Alkaline phosphatase is a zinc metalloprotein and contains four equivalents of zinc per mole of alkaline phosphatase (56, 66, 72). Alkaline phosphatase often contains one equivalent of magnesium per mole of alkaline phosphatase (56). Zinc and magnesium are often added to commercial purchased preparations of alkaline phosphatase. Zinc is required for activity of the enzyme (73), but magnesium is not and it only activates the enzyme (56). If the magnesium is removed, the enzyme will function as normal but will not produce as much product, but if the zinc is removed, then enzyme will lose all activity. Chelating compounds such as EDTA can irreversibly inhibit alkaline phosphatase by removing the zinc from the enzyme (17, 74, 75).

3.2 Experimental

3.2.1 Reagents

Alkaline phosphatase (EC 3.1.3.1 from calf intestine) was purchased from ICN Biomedicals (Aurora, OH). AttoPhos ([2,2'-bibenzothiazol]-6-hydroxy-benzathiazole phosphate) was obtained from Promega (Madison, WI). Sodium vanadate and diethanolamine (DEA) were supplied by Acros (Pittsburgh, PA). Disodium EDTA was purchased from Fisher Scientific. Sodium arsenate was supplied by Mallinckrodt (St. Louis, MO). All solutions and buffers were prepared in ultrapure water (>18 MΩ·cm, Barnstead E-pure System, Dubuque, IA).

3.2.2 Experimental Conditions

All experimental conditions for the assays by capillary electrophoresis and by the microplate reader presented in this chapter are identical to the experimental conditions described in detail in Chapter 2.2.2 and 2.2.3.

3.3 Results and Discussion

3.3.1 Alkaline Phosphatase Inhibition by Competitive, Reversible Inhibitors

Figure 3.1 presents the data for a capillary electrophoretic enzyme–inhibitor assay for sodium vanadate. Reversible inhibition of alkaline phosphatase by sodium vanadate is evident from these data when compared to Figure 2.2. Due to the greater mobility of alkaline phosphatase, sodium vanadate (75 μM) was injected first for 5.0 s at 17.8 kV (310 V/cm). Next a constant potential of 17.8 kV was applied for 50.0 s. Then 0.18 nM alkaline phosphatase was injected for 3.0 s at 17.8 kV. Since sodium vanadate is a reversible inhibitor, the resulting product plateau (Figure 3.1) is similar in appearance to the product plateau for theophylline inhibition as seen in Figure 2.3. All buffers were pH 9.5 and contained 50 mM diethanolamine and 0.10 mM AttoPhos. The electrophoretic currents were typically 10 μA.

According to the Michaelis–Menten treatment of a reversible, competitive inhibitor, V_{max} is unaffected by the inhibitor, but the apparent K_m, the Michaelis constant, will vary with inhibitor concentration. A Dixon plot can be used to

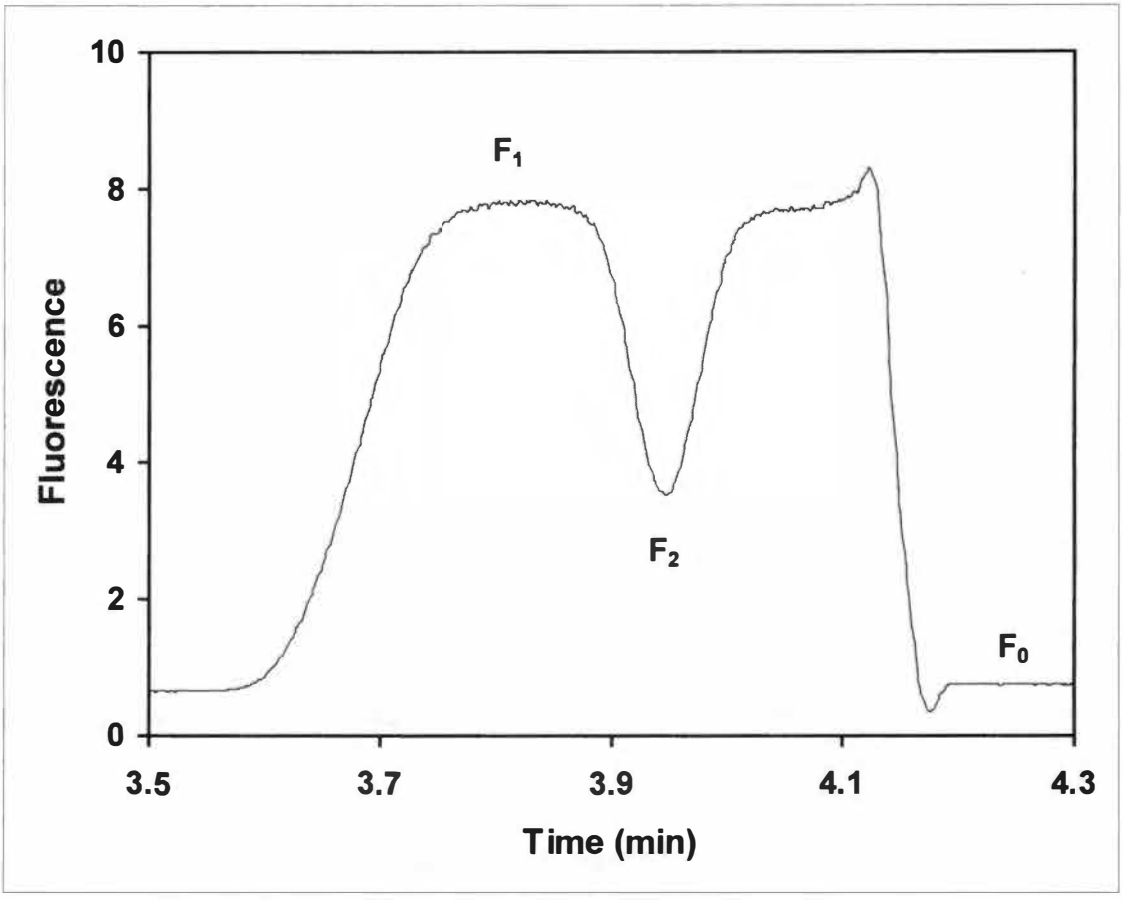

Figure 3.1. Electropherogram of a sodium vanadate–alkaline phosphatase enzyme–inhibitor assay

determine the K_i value of a competitive inhibitor (64). The equation used for the Dixon plot is as follows:

$$1/v = (K_m/V_{max}[S]K_i)[I] + 1/V_{max}(1+K_m/[S]) \quad (3a)$$

where v is the velocity of the reaction at inhibitor concentration, [I], V_{max} is the maximum velocity of the enzyme at the concentration of substrate in absence of inhibitor, [S] is the concentration of substrate, and K_i is the equilibrium constant of the inhibitor binding to the enzyme. A plot of $1/v$ versus [I] should be linear, and K_i can be determined from the slope and intercept of the line and V_{max}.

In order to generate a Dixon plot for sodium vanadate, an inhibitor response factor, RI_{ce}, was defined for the capillary electrophoresis experiments as follows:

$$RI_{ce} = (F_1 - F_0)/(F_2 - F_0) \quad (3b)$$

where F_1 (Figure 3.1) is proportional to the rate of product formation without inhibitor and is used to normalize the data due to variability in the height of the plateau from experiment to experiment. F_2 (Figure 3.1) is the minimum product formation observed in the plateau. F_0 is the baseline fluorescence (Figure 3.1). RI_{ce} is proportional to $1/v$ in Equation 3a. A similar approach was used to analyze theophylline in Chapter 2.3.3. In Figure 3.2, RI_{ce} values at different concentrations of sodium vanadate have been plotted. In order to determine K_i for sodium vanadate, V_{max} is required. V_{max} is determined from the RI_{ce} value of the capillary electrophoretic assay without inhibitor (Figure 2.1). The K_i was determined to be 2.1 ± 1.5 μM for sodium vanadate from the Dixon plot in Figure

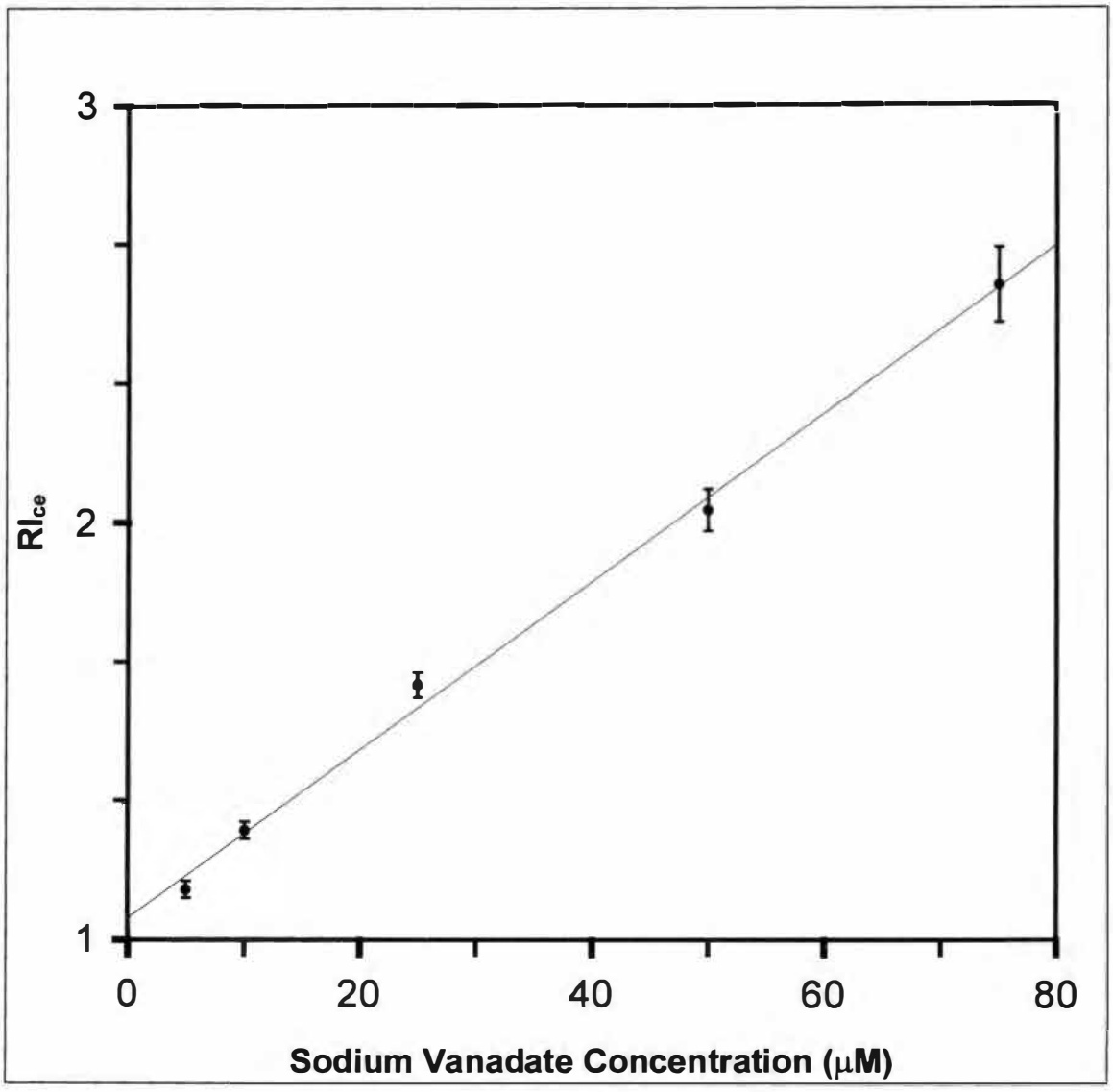

Figure 3.2. A plot of RI_{ce} versus sodium vanadate concentration

3.2 (R^2 = 0.997). The detection limit for sodium vanadate was 3 μM.

Microplate fluorometer experiments analogous to the capillary electrophoretic enzyme–inhibitor assays were performed. A response factor, RI_{mp}, for the microplate fluorometer was defined as $1/v$ where $1/v$ is the inverse of the initial velocity of the enzyme-catalyzed reaction. The slope of the plot of fluorescence versus time for the microplate experiments is used to determine v. Figure 3.3 shows the Dixon Plot, RI_{mp} versus concentration of sodium vanadate, for the microplate experiments. V_{max} is determined by carrying out experiments to generate a Lineweaver–Burk Plot as defined by the equation below (64):

$$1/v = (K_m/V_{max})(1/[S]) + 1/V_{max} \qquad (3c)$$

A plot of $1/v$ versus 1/[S] should be linear, and V_{max} can be determined from the inverse of the intercept. From the slope and intercept of the line and the V_{max} value, the K_i was determined to be 3.5 ± 0.2 μM for sodium vanadate (R^2 = 0.998). The analysis of the sodium vanadate data assumed steady-state kinetics, and comparison of the results from the capillary electrophoretic enzyme–inhibitor assays to the microplate assays, indicated that the capillary electrophoretic enzyme–inhibitor assays exhibited steady-state behavior. The K_i values for the capillary electrophoretic and microplate enzyme–inhibitor assays are in agreement with reported values (66, 67).

An electropherogram from a capillary electrophoretic enzyme–inhibitor assay of the reversible inhibition of alkaline phosphatase by sodium arsenate is presented in Figure 3.4. In this experiment, 125 μM sodium arsenate was injected first for 8.0 s at 17.8 kV (310 V/cm) since the enzyme-substrate complex

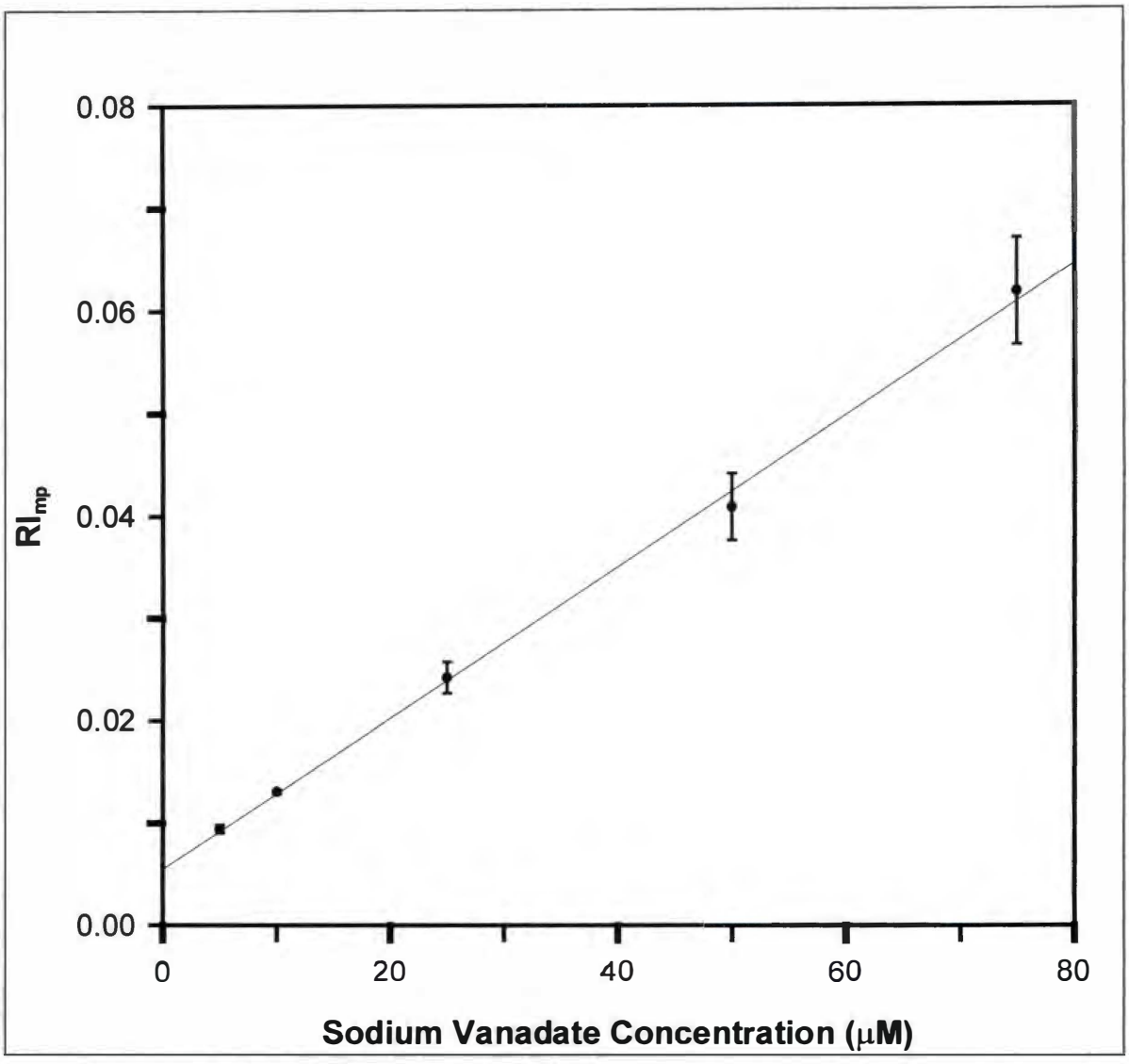

Figure 3.3. A plot of RI_{mp} versus the concentration of sodium vanadate

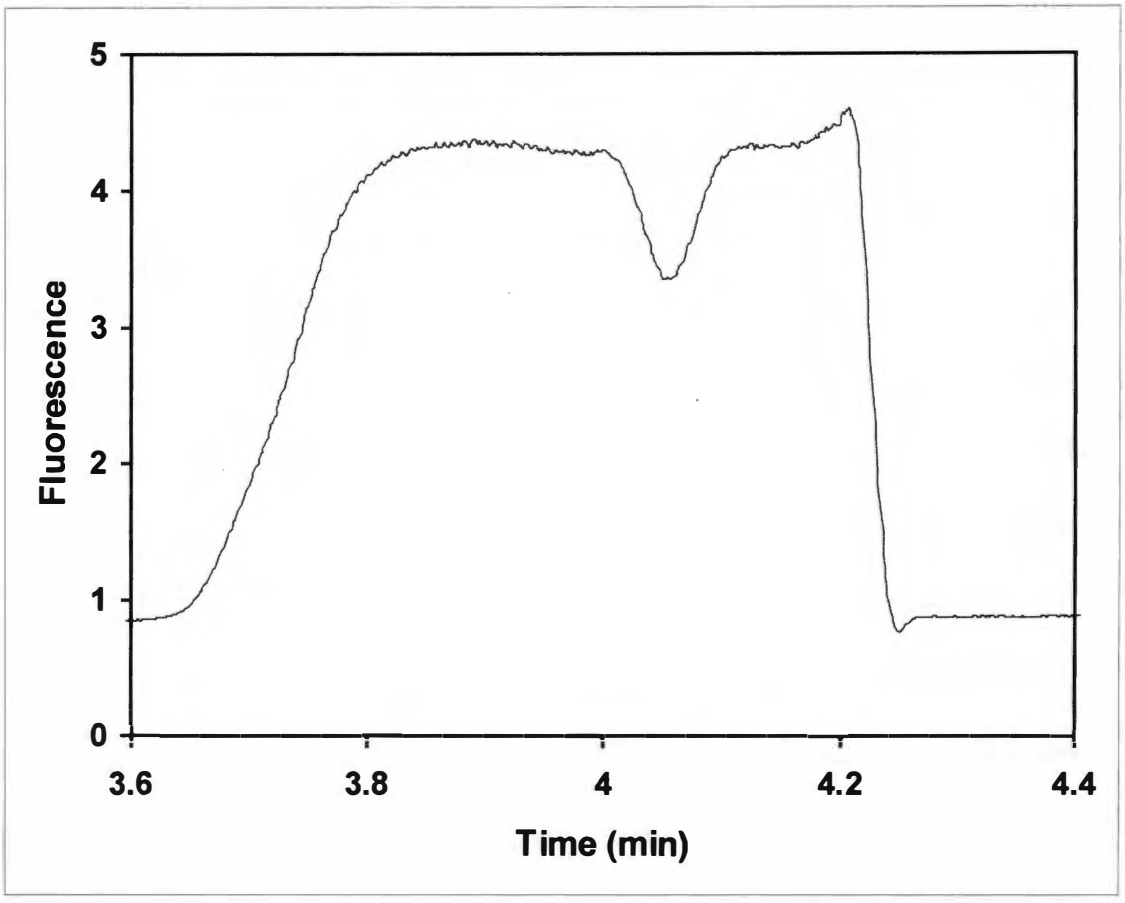

Figure 3.4. Electropherogram of a sodium arsenate-alkaline phosphatase enzyme-inhibitor assay

has a greater mobility than arsenate. Then a constant potential of 17.8 kV was applied for 150.0 s. Alkaline phosphatase (0.18 nM) was injected for 3.0 s at 17.8 kV before the application of the separation potential (17.8 kV). Since sodium arsenate is a reversible, competitive inhibitor, its response is similar to that for sodium vanadate.

The kinetic treatment of the capillary electrophoretic enzyme–inhibitor assay data for sodium arsenate was the same as for sodium vanadate. The plot of RI_{ce} at different concentrations of sodium arsenate (25 to 250 μM; N = 3) was linear (R^2 = 0.999), indicating that the arsenate assays exhibited steady-state behavior. The K_i for sodium arsenate was 21 ± 4 μM. Microplate fluorometer experiments were performed for sodium arsenate, and the kinetic treatment of the data was the same as for sodium vanadate. The K_i for sodium arsenate for the microplate fluorometer was determined to be 8.6 ± 1.4 μM. The K_i values for the CE and microplate fluorometer enzyme–inhibitor assays are in agreement with reported values for sodium arsenate. It is unclear why the K_i value determined for sodium arsenate using CE is a factor of two higher than the K_i determined using microplate experiments. This could be a kinetic effect since the electrophoretic experiment takes place on a faster time scale than the microplate experiments. However, the capillary electrophoretic data for sodium arsenate gave an excellent fit to the equation for the Dixon plot, and the K_i values obtained for other reversible inhibitors (vanadate and theophylline) were similar using both techniques.

3.3.2 Alkaline Phosphatase Inhibition by an Irreversible Inhibitor

Alkaline phosphatase is a zinc metalloprotein and contains four equivalents of zinc per mole of alkaline phosphatase (56, 66, 72). Zinc is required for activity of the enzyme (73). Chelating compounds such as EDTA can irreversibly inhibit alkaline phosphatase by removing the zinc from the enzyme (17, 74, 75). A capillary electrophoretic enzyme–inhibitor assay indicating irreversible inhibition of alkaline phosphatase by EDTA is shown in Figure 3.5. In this experiment, 1.0 mM EDTA was injected first for 55.0 s at 17.8 kV (310 V/cm). Next a constant potential of 17.8 kV was applied for 180.0 s. Then 0.18 nM alkaline phosphatase was injected for 3.0 s at 17.8 kV. As presented in Figure 3.5, product formation decreased when the zones of inhibitor and enzyme–substrate complex mixed electrophoretically (4.2 min, Figure 3.5). After the zones of inhibitor and enzyme–substrate complex separated, the enzyme did not return to its original activity (4.0 min, Figure 3.5), indicating that the enzyme was irreversibly inhibited. The same experiment using 0.030 mM EDTA is presented in Figure 3.6. At this EDTA concentration, when the enzyme–substrate complex and inhibitor separated, the enzyme was activated rather than irreversibly inhibited.

In order to quantify to what extent alkaline phosphatase was irreversibly inhibited or activated by EDTA, the ratio of enzyme activity before and after the enzyme interacted with EDTA was measured over a range of EDTA concentrations. The fractional activity is calculated as follows:

$$\textit{fractional activity} = (I_1 - I_0)/(I_2 - I_0) \qquad (3d)$$

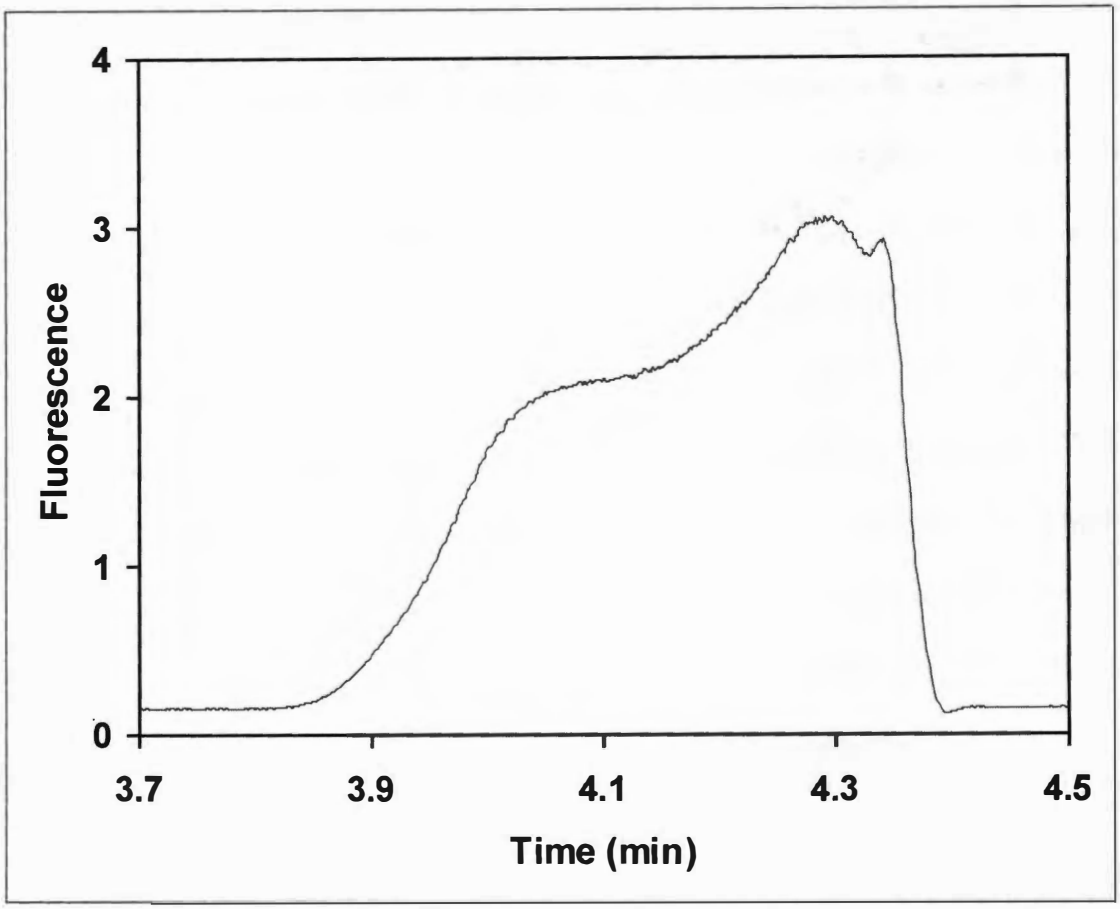

Figure 3.5. Electropherogram of an EDTA-alkaline phosphatase enzyme-inhibitor assay

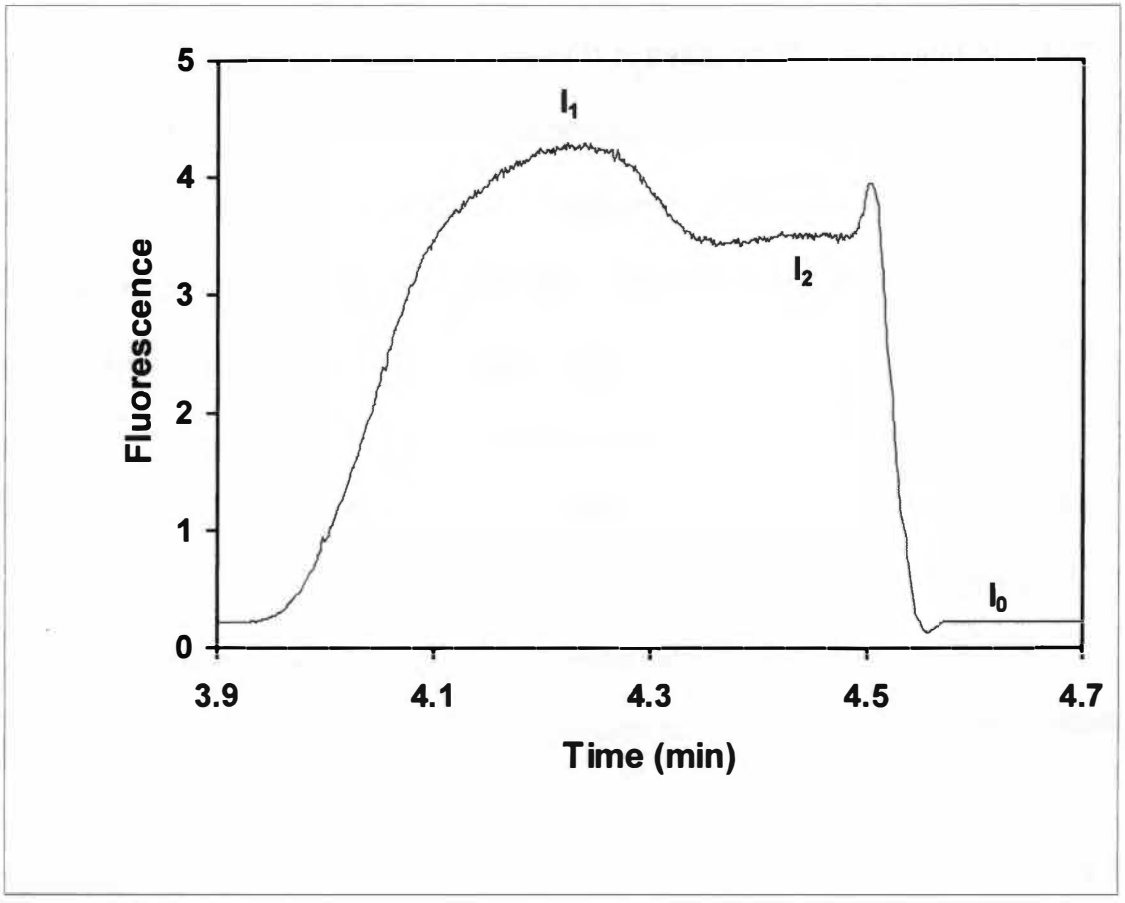

Figure 3.6. Activation of alkaline phophatase by 0.030 mM EDTA

where I_1 (Figure 3.6) is the activity of alkaline phosphatase after interacting with EDTA, I_2 is the activity of alkaline phosphatase before interacting with EDTA, and I_0 is the baseline fluorescence. Figure 3.7 presents the fractional activity versus EDTA concentration from 10 μM to 4.0 mM. The dotted line is the fractional activity measured for control assays (Figure 2.2). Fractional activity values above this line indicate inhibition. Concentrations of EDTA at 1.0 mM and higher irreversibly inhibit alkaline phosphatase. Concentrations from 20 to 400 μM EDTA activate alkaline phosphatase. The maximum activation is observed at 40 μM. EDTA is thought to irreversibly inhibit alkaline phosphatase by binding to the zinc bound to the enzyme and then removing the zinc, leaving the enzyme inactivated (17, 75). The mechanism by which EDTA activates alkaline phosphatase is unknown.

Activation of alkaline phosphatase by EDTA has been reported for human placental alkaline phosphatase at concentrations of 10 to 100 mM EDTA (16), for *Gastrothylax crumenifer and Cotylophoron orientale* alkaline phosphatases at 1.0 mM EDTA (76), and for *Ascaris suum* alkaline phosphatase at 10 mM EDTA (77). However, the alkaline phosphatases used in all three of these studies were in crude preparations, and it was not clear what other enzymes were present in these preparations. Only one alkaline phosphatase was from a mammalian source (human placental), and this showed inhibition at low EDTA concentrations (10 μM to 1mM) and activation at high EDTA concentrations (10 to 100 mM). This was the opposite of what is observed here for calf intestinal alkaline

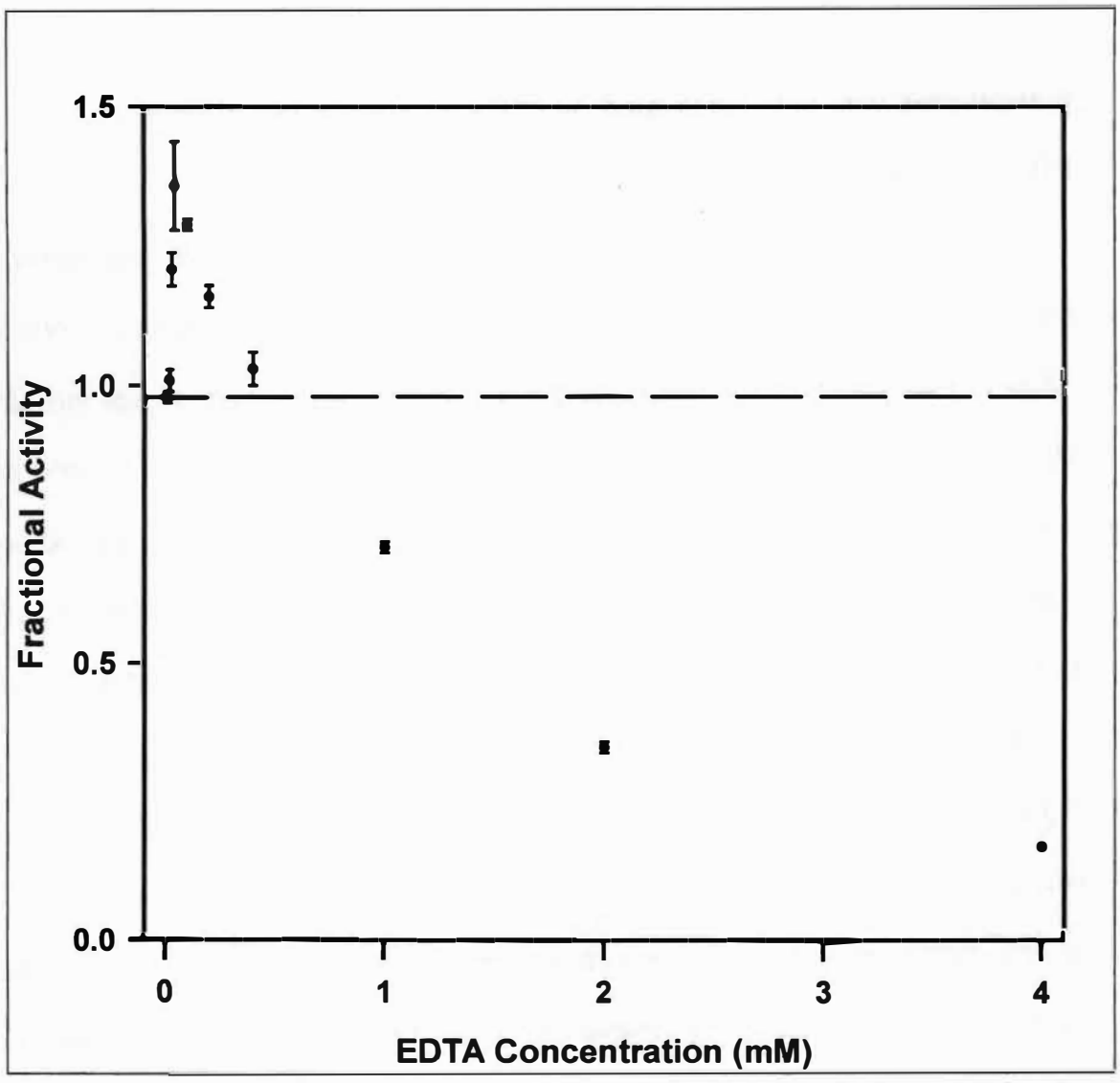

Figure 3.7. A plot of fractional activity versus concentration

phosphatase where activation was observed at low EDTA concentrations (20 to 400 μM), and inhibition was observed at high EDTA concentrations (1.0 mM or higher). It has also been reported that purified human placental alkaline phosphatase was only inactivated by EDTA (5 to 40 mM) and not activated by EDTA at any concentration (78).

One possible explanation for these results, unrelated to the ability of EDTA to chelate zinc, is ionic strength effects of the EDTA injection zone on alkaline phosphatase (79, 80). In order to determine whether or not the ionic strength of the EDTA zone was causing the observed irreversible inhibition and activation of alkaline phosphatase, the same experiments were performed with sodium chloride replacing EDTA. The ionic strength of the sodium chloride solutions is the same as the EDTA solutions used in the experiments presented in Figure 3.7. A plot of fractional activity versus ionic strength is presented in Figure 3.8. The open circles represent the fractional activity for EDTA, and the closed circles represent the fractional activity for sodium chloride. The dotted line is the fractional activity measured for control assays (Figure 2.2). These experiments indicate that the change in ionic strength due to EDTA does not cause the observed inhibition of alkaline phosphatase. However, the activity increase is less than that observed for EDTA at all ionic strengths. For example, at an ionic strength of 0.66 mM, the fractional activity of the enzyme increased by 4% for sodium chloride and increased by 32% for EDTA. At an ionic strength of 1.32 mM, the fractional activity of the enzyme increased by 4% for sodium chloride and increased by 18 % for EDTA. At an ionic strength of 26.5 mM, the

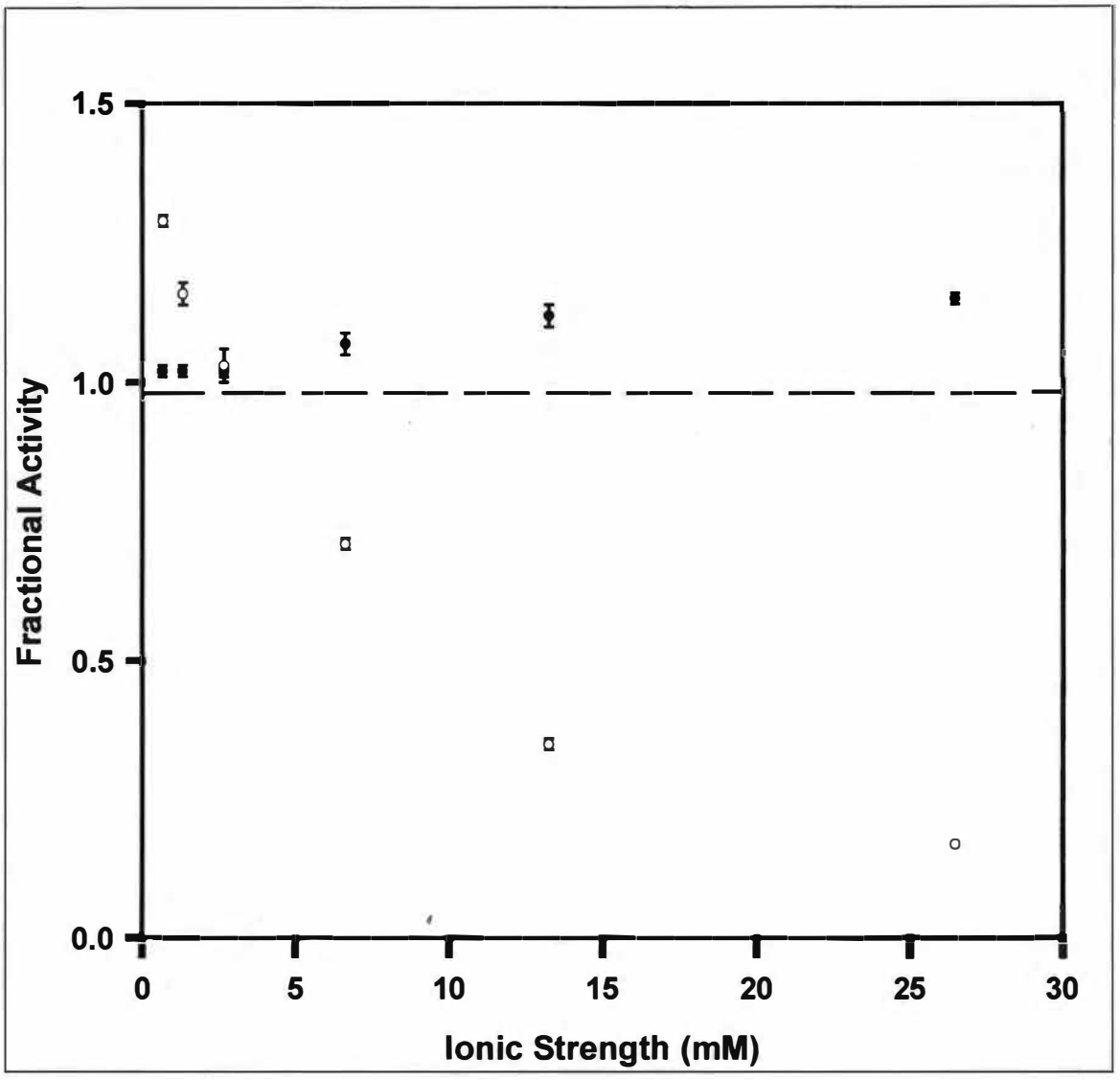

Figure 3.8. A plot of fractional activity versus ionic strength. The open circles represent the fractional activity for EDTA, and the closed circles represent the fractional activity for sodium chloride.

fractional activity of the enzyme increased by 17% for sodium chloride and decreased by 83% for EDTA. It has been reported that the addition of some salts, including sodium chloride, increases the activity of *E. coli* alkaline phosphatase (80). However, activation of the magnitude observed at low EDTA concentrations here cannot be attributed to only ionic strength.

Chapter 4

Conclusions and Future Work

4.1 Conclusions

An on-column capillary electrophoretic enzyme-inhibition assay has been developed to study different types of inhibition, reversible and irreversible, and activation. Competitive and noncompetitive reversible inhibitors can be analyzed quantitatively using Michaelis–Menten treatment of the capillary electrophoretic data. Fractional activity of irreversible inhibitors and activators can also be determined. Using this approach, reversible inhibition, irreversible inhibition and activation can be readily distinguished by only visual inspection of single electropherograms and comparison to control electropherograms.

The inhibition of alkaline phosphatase by the noncompetitive, reversible inhibitor, theophylline, was studied using capillary electrophoresis. The calculated K_i for theophylline is 102 ± 4 μM for the capillary electrophoretic enzyme–inhibition assays and is in agreement with literature values. The inhibition of alkaline phosphatase by the competitive reversible, inhibitors sodium vanadate and sodium arsenate resulted in calculated K_i values of 2.1 ± 1.5 μM and 21 ± 4 μM for the capillary electrophoretic enzyme–inhibition assays. The K_i values determined for vanadate and arsenate using the CE method are consistent with values determined using traditional enzyme assays in a microplate reader and

with literature values. Irreversible inhibition as well as activation by EDTA was observed for the capillary electrophoretic enzyme-inhibition assays.

Only 1.9 attomoles of alkaline phosphatase was required for the CE experiment, whereas 36 femtomoles of alkaline phosphatase was required for analogous experiments using a microplate fluorometer (200 μL sample volume). The capillary electrophoretic enzyme-inhibition assays give more information per experiment as compared to traditional methods including the microplate enzyme-inhibition assays as well as consuming less enzyme per experiment (10^4 less compared to microplate experiments). From visual inspection alone, the type of inhibition (reversible or irreversible) or activation can easily be identified. Other information is also provided from the electropherogram that traditional enzyme assays do not provide. Traditional methods allow one to see the activity of the enzyme while it is interacting with the inhibitor, but the capillary electrophoretic assays allow one to see the activity of the enzyme before interacting with the inhibitor or activator, the activity of the enzyme while it interacts with the inhibitor, and the activity of the enzyme after interacting with the inhibitor. The capillary-electrophoretic assays provide greater insight of the enzyme activity after being separated from the inhibitor or activator that traditional methods do not allow. Other information can also be obtained from the electropherogram of an enzyme-inhibition assay including velocity of the enzyme–substrate complex, product, and inhibitor, the time the inhibitor and enzyme interact, and where in the capillary the enzyme and inhibitor interact (equations are in the Appendix).

Inhibition and activation of alkaline phosphatase has been observed using the developed capillary electrophoretic enzyme-inhibition assays.

4.2 Future Studies

Future studies should include studying the mechanism of the EDTA inhibition and activation by developing more mathematical descriptions of these assays to expand the quantitative information that can be obtained from the electropherograms. Microplate assays can also be performed with EDTA to gather more information about how EDTA interacts with alkaline phosphatase. The data obtained from the microplate should be further analyzed by mathematical treatment of irreversible inhibition kinetics that has been reported in the literature (18, 81). Also the mechanism of the EDTA inhibition and activation should be compared to other similar chelators. Some possibilities of chelators are ethylene glycol-bis(2-aminoethyl)-*N*,*N*,*N*′,*N*′-tetraacetic acid (EGTA), nitriloacetic acid (NTA), and 1,10-phenanthroline. Comparison of the fractional activity of these to the fractional activity of EDTA will provide insight to how chelators interact with alkaline phosphatase on a short time scale. Reactivation of alkaline phosphatase after interact with EDTA or other chelators can also be explored by injecting a separate zone of Zn^{+2} along with the zones of EDTA (or other chelator) and alkaline phosphatase. Activation of alkaline phosphatase by reported activators in the literature should also be explored (56). From preliminary data, sodium cyanide and cysteine are promising activators to study. Studying the theoretical interaction times versus the experimentally determined

interaction times of the inhibitor and enzyme by using the derived equations in the Appendix should be compared in order to describe how the enzyme and inhibitor interact in the capillary. Other enzymes and their important inhibitors should also be studied to demonstrate the versatility of these enzyme–inhibition assays developed here.

References

References

(1) Zubay, G. L. *Biochemistry*, 4th ed.; Wm. C. Brown Publishers: Dubuque, IA, 1996.

(2) Lehninger, A. L.; Nelson, D. L.; Coxq, M. M. *Principles of Biochemistry*, 2nd ed.; Worth Publishers, Inc.: New York, 1993.

(3) Tipton, K. F. In *Enzyme Assays*; Eisenthal, R., Danson, M. J., Eds.; IRL press: Oxford, 1992, pp 1-53.

(4) John, R. A. In *Enzyme Assays*; Eisenthal, R., Danson, M. J., Eds.; IRL Press: Oxford, 1992, pp 59-91.

(5) Weitzman, P. D. J.; Watkins, P. J. In *Enzyme Assays*; Eisenthal, R., Danson, M. J., Eds.; IRL Press: Oxford, 1992, pp 167-178.

(6) Clark, J. B. In *Enzyme Assays*; Eisenthal, R., Danson, M. J., Eds.; IRL Press: Oxford, 1992, pp 181-190.

(7) Brocklehurst, K. In *Enzyme Assays*; Eisenthal, R., Danson, M. J., Eds.; IRL Press: Oxford, 1992, pp 191-214.

(8) Harmon, B. J.; Patterson, D. H.; Regnier, F. E. *J. Chromatogr. A* **1993,** *657*, 429-434.

(9) Hilder, V. A.; Boulter, D. *Crop Protect.* **1999,** *18*, 177-191.

(10) Gatehouse, A. M. R.; Gatehouse, J. A. *Pestic. Sci.* **1998,** *52*, 165-175.

(11) Palfreyman, M. G.; McCann, P. P.; Lovenberg, W.; Joseph G. Temple, J.; Sjoerdsma, A. *Enzymes as Targets for Drug Design*; Academic Press, Inc.: San Diego, 1989.

(12) Sandler, M. *Enzyme Inhibitors as Drugs*; The Macmillan Press Limited: London, 1980.

(13) Louie, A. Y.; Meade, T. J. *Chem. Rev.* **1999,** *99*, 2711-2734.

(14) Krawczyk, T. K. v. *Chem. Anal.* **1998,** *43*, 135-158.

(15) Ochs, R. S. *J. Chem. Educ.* **2000,** *77*, 1453-1456.

(16) Conyers, R. A. J.; Birkett, D. J.; Neale, F. C.; Posen, S.; Brudenell, J. *Biochim. Biophys. Acta* **1967,** *139*, 363-371.

(17) Ackermann, B. P.; Ahlers, J. *Biochem. J.* **1976,** *153*, 151-157.

(18) Chen, Q.-X.; Zhang, W.; Wang, H.-R.; Zhou, H.-M. *Int. J. Biol. Macromol.* **1996,** *19*, 257-261.

(19) Zhang, R.-Q.; Chen, Q.-X.; Li-Ping, R. X.; Zeng, X.-G.; Zhou, H.-M. *Biochim. Biophys. Acta* **2001,** *1545.*

(20) Bao, J. J.; Fujima, J. M.; Danielson, N. D. *J. Chromatogr. B* **1997,** *699*, 481-497.

(21) Schultz, N. M.; Tao, L.; Rose, D. J.; Kennedy, R. T. In *Handbook of Capillary Electrophoresis*; Landers, J. P., Ed.; CRC Press: Boca Raton, 1997, pp 611-637.

(22) Craig, D. B.; Arriaga, E. A.; Wong, J. C. Y.; Lu, H.; Dovichi, N. J. *J. Am. Chem. Soc.* **1996,** *118*, 5245-5253.

(23) Xue, Q.; Yeung, E. S. *Nature* **1995,** *373*, 681-683.

(24) Xue, Q.; Yeung, E. S. *Anal. Chem.* **1994,** *66*, 1175-1178.

(25) Bao, J.; Regnier, F. E. *J. Chromatogr.* **1992,** *608*, 217-224.

(26) Harmon, B. J.; Patterson, D. H.; Regnier, F. E. *Anal. Chem.* **1993,** *65*, 2655-2662.

(27) Cohen, C. B.; Chin-Dixon, E.; Jeong, S.; Nikiforov, T. T. *Anal. Biochem.* **1999,** *273*, 89-97.

(28) Hadd, A. G.; Raymond, D. E.; Halliwell, J. W.; Jacobson, S. C.; Ramsey, J. M. *Anal. Chem.* **1997,** *69*, 3407-3412.

(29) Hadd, A. G.; Jacobson, S. C.; Ramsey, J. M. *Anal. Chem.* **1999,** *71*, 5206-5212.

(30) Xu, Y.; Liu, X.; Ip, M. P. C. *J. Liq. Chromatogr. Relat. Technol.* **1998,** *21*, 2781-2797.

(31) Saevels, J.; Schepdael, A. V.; Hoogmartens, J. *Electrophoresis* **1996,** *17*, 1222-1227.

(32) Chang, H.-T.; Yeung, E. S. *Anal. Chem.* **1993,** *65*, 2947-2951.

(33) Saevels, J.; Huygens, K.; Schepdael, A. V.; Hoogmartens, J. *Anal. Chem.* **1997,** *69*, 3299-3303.

(34) Harmon, B. J.; Regnier, F. E. *Chem. Anal.* **1998,** *146*, 925-943.

(35) Regnier, F. E.; Patterson, D. H.; Harmon, B. J. *Trends Anal. Chem.* **1995,** *14*, 177-181.

(36) Avila, L. Z.; Whitesides, G. M. *J. Org. Chem.* **1993,** *58*, 5508-5512.

(37) Zhang, Y.; El-Maghrabi, M. R.; Gomez, F. A. *Analyst* **2000,** *125*, 685-688.

(38) Dyck, S. V.; Schepdael, A. V.; Hooigmartens, J. *Electrophoresis* **2002,** *23*, 2854-2859.

(39) Dyck, S. V.; Schepdael, A. V.; Hoogmartens, J. *Electrophoresis* **2002,** *23*, 1341-1347.

(40) Murakami, Y.; Morita, T.; Kanekiyo, T.; Tamiya, E. *Biosens. Bioelectron.* **2001,** *16*, 1009-1014.

(41) Kanie, Y.; Kanie, O. *Carbohyd. Res.* **2002,** *337*, 1757-1762.

(42) Kanie, Y.; Kanie, O. *Electrophoresis* **2003,** *24*, 1111-1118.

(43) Dyck, S. V.; Schepdael, A. V.; Hoogmartens, J. *Electrophoresis* **2001,** *22*, 1436-1442.

(44) Bousse, L.; Cohen, C.; Nikiforov, T.; Chow, A.; Kopf-Sill, A. R.; Dubrow, R.; Parce, J. W. *Annu. Rev. Biophys. Biomol. Struct.* **2000,** *29*, 155-181.

(45) Wang, J.; Chatrathi, M. P.; Tian, B.; Polsky, R. *Anal. Chem.* **2000,** *72*, 2514-2518.

(46) Wang, J.; Chatrathi, M. P.; Tian, B. *Anal. Chem.* **2001,** *73*, 1296-1300.

(47) Zugel, S. A.; Burke, B. J.; Regnier, F. E.; Lytle, F. E. *Anal. Chem.* **2000,** *72*, 5731-5735.

(48) Olsen, K.; Otte, J.; Skibsted, L. H. *J. Agric. Food Chem.* **2000,** *48*, 3086-3089.

(49) Takebayashi, M.; Hiranuma, S.; Kanie, Y.; Kajimoto, T.; Kanie, O.; Wong, C.-H. *J. Org. Chem.* **1999,** *64*, 5280-5291.

(50) Kanie, Y.; Kirsch, A.; Kanie, O.; Wong, C.-H. *Anal. Biochem.* **1998,** *263*, 240-245.

(51) Bhoopathy, S.; Sarkar, M.; Karnes, H. T. *J. Pharm. Biomed. Anal.* **2001,** *25*, 721-729.

(52) Starkey, D. E.; Han, A.; Bao, J. J.; Ahn, C. H.; Wehmeyer, K. R.; Prenger, M. C.; Halsall, H. B.; Heineman, W. R. *J. Chromatogr. B* **2001,** *762*, 33-41.

(53) Wang, J.; Chatrathi, M. P.; Ibanez, A. *Analyst* **2001,** *126*, 1203-1206.

(54) Saevels, J.; Steen, K. V. d.; Schepdael, A. V.; Hoogmartens, J. *J. Chromatogr. A* **1996,** *745*, 293-298.

(55) Novakova, S.; Telnarova, M.; Glatz, Z. *J. Chromatogr. A* **2003,** *990*, 189-195.

(56) McComb, R. B.; Bowers, G. N.; Posen, S. *Alkaline Phosphatase*; Plenum Press: New York, 1979.

(57) Jourquin, G.; Kauffmann, J. M. *J. Pharm. Biomed. Anal.* **1998,** *18*, 585-596.

(58) Vinet, B.; Zizian, L.; Gauthier, B. *Clin. Biochem.* **1978,** *11*, 57-61.

(59) Vassallo, R.; Lipsky, J. J. *Mayo Clin. Proc.* **1998,** *73*, 346-354.

(60) Page, C. P. *J. Clin. Pharmacol.* **1999,** *39*, 237-240.

(61) Markham, A.; Faulds, D. *Drugs* **1998,** *56*, 1081-1091.

(62) Wu, D.; Regnier, F. E.; Linhares, M. C. *J. Chromatogr. B* **1994,** *657*, 357-363.

(63) Craig, D. B.; Wong, J. C. Y.; Dovichi, N. J. *Anal. Chem.* **1996,** *68*, 697-700.

(64) Segel, I. H. *Enzyme Kinetics*; John Wiley and Sons: New York, 1975.

(65) Curti, C.; Pizauro, J. M.; Ciancaglini, P.; Leone, F. A. *Cell. Mol. Biol.* **1987,** *33*, 625-635.

(66) Holtz, K. M.; Stec, B.; Kantrowitz, E. R. *J. Biol. Chem.* **1999,** *274*, 8351-8354.

(67) Shirazi, S. P.; Beechey, R. B.; Butterworth, P. J. *Biochem. J.* **1981,** *194*, 803-809.

(68) Tracey, A. S.; Crans, D. C. ; American Chemical Society: Washington, D. C., 1998; Vol. 711.

(69) Sekar, N.; Li, J.; Shechter, Y. *Crit. Rev. Biochem. Mol. Biol.* **1996,** *31*, 339-359.

(70) Badmaev, V.; Prakash, S.; Majeed, M. *J. Altern. Complem. Med.* **1999,** *5*, 273-291.

(71) Lin, J.-K.; Shao, T.-H.; Hwang, J.-Y. *J. Chin. Biochem. Soc.* **1973,** *2*, 52-63.

(72) Butterworth, P. J. *Cell. Biochem. Func.* **1983,** *1*, 66-70.

(73) Bortolato, M.; Besson, F.; Roux, B. *Proteins: Struct. Funct. Genet.* **1999,** *37*, 310-318.

(74) Fortuna, R.; Anderson, H. C.; Carty, R.; Sajdera, S. W. *Biochim. Biophys. Acta* **1979,** *570*, 291-302.

(75) Ensinger, H. A.; Pauly, H. E.; Pfleiderer, G.; Stiefel, T. *Biochim. Biophys. Acta* **1978,** *527*, 432-441.

(76) Gupta, P. C.; Bahadur, R. *Indian Vet. Med. J.* **1984,** *8*, 164-170.

(77) Butterworth, J.; Probert, A. J. *Exp. Parasitol.* **1970,** *28*, 557-565.

(78) Miggiano, G. A. D.; Pileri, M.; Mordente, A.; Martorana, G. E.; Castelli, A. *Clin. Chim. Acta* **1985,** *145*, 331-336.

(79) Quirino, J. P.; Terabe, S. *J. Chromatogr. A* **2000,** *902*, 119-135.

(80) Poe, R. W.; Sangadala, V. S.; Brewer, J. M. *J. Inorg. Biochem*. **1993,** *15*, 173-180.

(81) Zhang, R.-Q.; Chen, Q.-X.; Xiao, R.; Xie, L.-P.; Zeng, X.-G.; Zhou, H.-M. *Biochim. Biophys. Acta* **2001,** *1545*, 6-12.

Appendix

Appendix

Quantitative Information Obtained From Enzyme-Inhibition Electropherograms

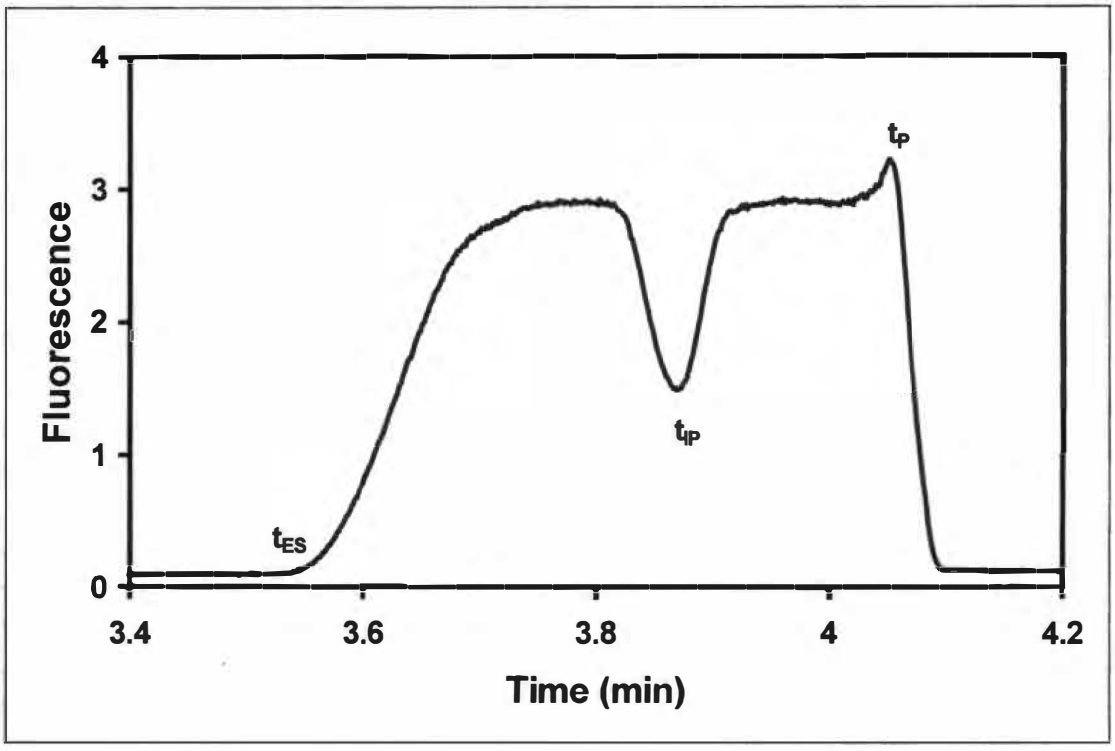

Figure A.1. Electropherogram with relative times noted for calculation of quantitative information

Defined Variables

d = distance from the injection end where the enzyme and inhibitor interact

L_d = distance to the detector window

t = time that the enzyme and inhibitor interact

t_{ES} = time that the enzyme-substrate complex is detected as it migrates past the detector window

t_{IP} = time that the inhibition product is detected

t_P = time that that the first product formed

$\Delta t_{E\&I}$ = time difference between the injection of the inhibitor and the enzyme

v_{ES} = velocity of the enzyme-substrate complex = L_d/t_{ES}

v_I = velocity of the inhibitor

v_P = velocity of the product = L_d/t_P

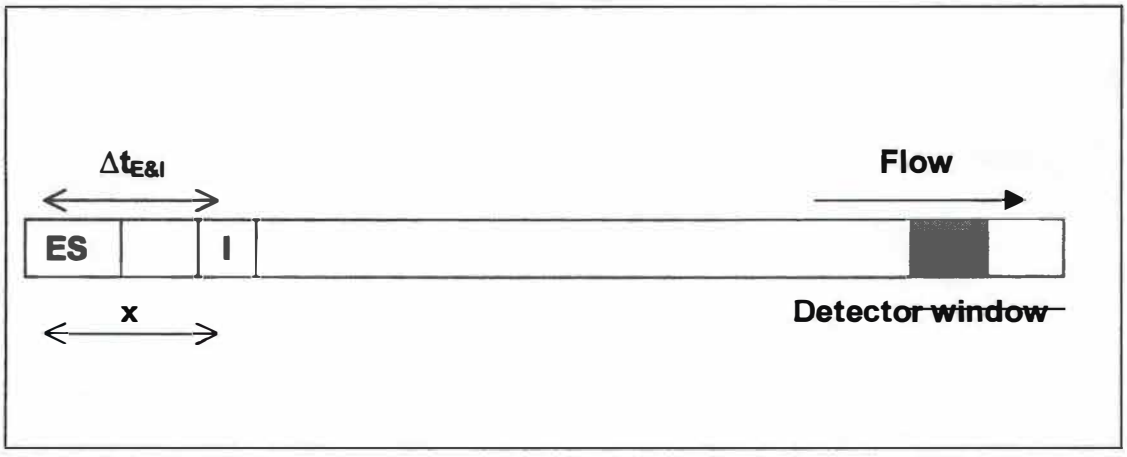

Figure A.2. A cross view of a capillary and the relative positioning of the inhibitor and enzyme-substrate complex zones

In the experiments presented here, the inhibitor zone is always injected first because it has a lower mobility than the enzyme-substrate (ES) complex zone. The inhibitor zone will migrate through the capillary for some given time, $\Delta t_{E\&I}$, and will travel some distance, x, before the enzyme is injected. The enzyme is then injected at $\Delta t_{E\&I}$ (Figure A.2).

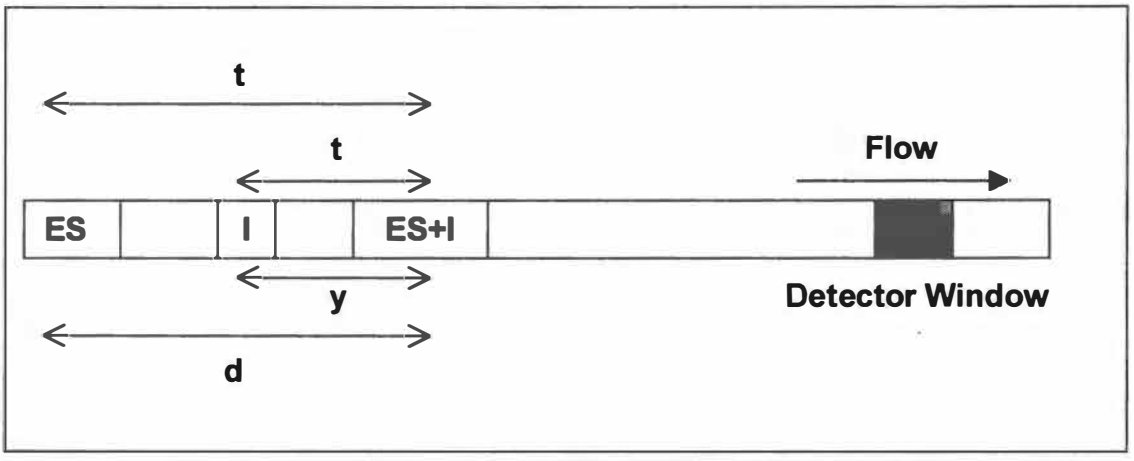

Figure A.3. A cross view of a capillary showing how far and how long the enzyme-substrate complex and inhibitor zones travel after the enzyme is injected in order for the zones to mix electrophoretically

As seen in Figure A.3, the inhibitor zone and the ES complex zone will travel the same time, t, to electrophoretically mix in the capillary. The ES complex zone travels the distance, d, to meet the inhibitor zone, and the distance, y, is how far the the inhibitor zone travels when the ES complex zone meets the inhibitor

zone. We can derive the exact time, t, that the ES complex zone and inhibitor zone mix electrophoretically. Below is the derivation.

We know the following equations based Figures A.2 and A.3 above:

$d = x + y \qquad x = v_I \bullet \Delta t_{E\&I} \qquad y = t \bullet v_I \qquad d = t \bullet v_{ES}$

We know that $d = x + y$ and $d = t \bullet v_{ES}$. Both can be set equal to each other as follows:

$$t \bullet v_{ES} = x + y \tag{Aa}$$

Substitute in $x = v_I \bullet \Delta t_{E\&I}$ into Equation Aa.

$$t \bullet v_{ES} = v_I \bullet \Delta t_{E\&I} + y \tag{Ab}$$

Substitute in $y = t \bullet v_I$ into Equation Ab.

$$t \bullet v_{ES} = v_I \bullet \Delta t_{E\&I} + t \bullet v_I \tag{Ac}$$

Rearrange Equation Ac and solve for t.

$$t\,(v_{ES} - v_I) = v_I \bullet \Delta t_{E\&I} \tag{Ad}$$

Equation 1: Time that the inhibitor and enzyme interact

$$\mathbf{t = (v_I \bullet \Delta t_{E\&I})/(v_{ES} - v_I)}$$

We must also solve for the time, t, where the enzyme and inhibitor zones mix electrophoretically in the capillary based on the time that the inhibition product (IP), t_{IP}, appears in the electropherogram. This will simplify the calculations.

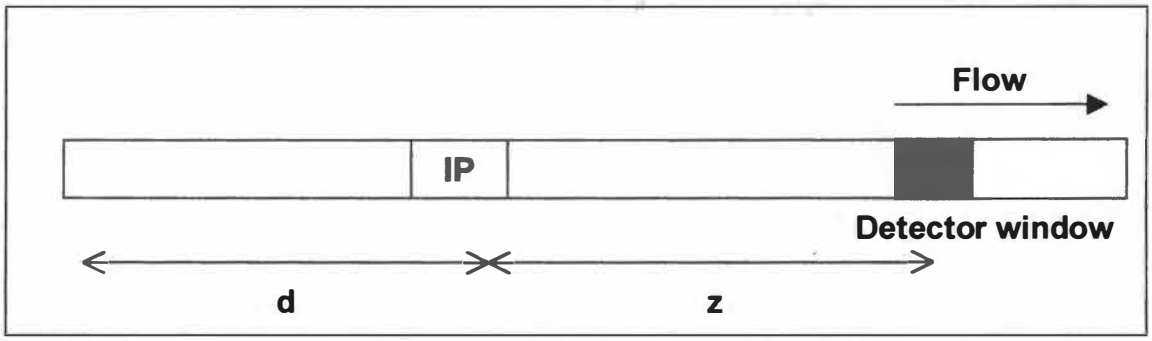

Figure A.4. Distance traveled by the inhibition product, IP

The inhibition product, IP, is formed where the ES complex and inhibitor zones mixed electrophoretically at the distance, d. The IP zone travels the distance, z, over the time, t_{IP}^*, to be detected at the detector window. The ES complex zone travels the distance, z, over time t_{ES}^*, to be detected at the detector window. We know the following based on Figure A.4:

$d + z = L_d$ $\quad z = t_{ES}^* \bullet v_{ES}$ $\quad z = t_{IP}^* \bullet v_P$

We can set the two equations above that each equal z equal to each other as follows:

$$t_{ES}^* \bullet v_{ES} = t_{IP}^* \bullet v_P \qquad \text{(Ae)}$$

We know that the total time that the ES complex zone migrates through the capillary is equal to the following:

$$t_{ES} = t + t_{ES}^* \qquad \text{(Af)}$$

The Equation Af can be rearranged to solve for t_{ES}^* substituted into Equation Ae as follows:

$$(t_{ES} - t)\, v_{ES} = t_{IP}^* \bullet v_P \qquad \text{(Ag)}$$

The total time required to observe the inhibition product, t_{IP}, is equal to the following:

$$t_{IP} = t + t_{IP}^{*} \qquad \text{(Ah)}$$

The Equation Ah can be rearranged to solve for t_{IP}^{*} and substituted into Equation Ag as follows:

$$(t_{ES} - t)\, v_{ES} = (t_{IP} - t)\, v_P \qquad \text{(Ai)}$$

Rearrange Equation Ai and solve for t.

$$t = (t_{IP} \bullet v_P - t_{ES} \bullet v_{ES}) / (v_P - v_{ES}) \qquad \text{(Aj)}$$

Equation Aj can be simplified down to an equation to solve for the time that the inhibition product is formed by only requiring the times t_{ES}, t_P, and t_{IP} from the electropherogram (Figure A.1). Substitute the following into Equation Aj:

$$v_{ES} \bullet t_{ES} = L_d \qquad v_P = L_d / t_P \qquad v_{ES} = L_d / t_{ES}$$

After the substitutions into Equation Aj and simplifying, the following equation results:

Equation 2: Time the inhibition product forms

$$\mathbf{t = [t_{ES} (t_{IP} - t_P)] / (t_{ES} - t_P)}$$

We can also determine the velocity of the inhibitor, v_I. We know the following based in Figure A.2:

$$v_I = y / t \qquad \text{(Ak)}$$

Substitute $y = d - x$ into Equation Ak.

$$v_I = (d - x) / t \qquad \text{(Al)}$$

Substitute $x = v_I \bullet \Delta t_{E\&I}$ into Equation AI.

$$v_I = (d - v_I \bullet \Delta t_{E\&I}) / t \qquad \text{(Am)}$$

Substitute $d = v_{ES} \bullet t$ into Equation Am.

$$v_I = (v_{ES} \bullet t - v_I \bullet \Delta t_{E\&I}) / t \qquad \text{(An)}$$

Rearrange Equation An, solve for v_I, and the following equation results:

Equation 3: Velocity of inhibitor zone

$$\mathbf{v_I = (v_{ES} \bullet t) / (t + \Delta t_{E\&I})}$$

From equations 1-3 and the times from the electropherogram from Figure A.1, the times and velocity of each zone (ES complex zone, inhibitor zone, and inhibition product) can be determined.

Vita

Angela Randall Whisnant was born in June 1974 in Morganton, NC. For a few years, she was raised in Lincolnton, NC where she attended school at Union Elementary School in Vale, NC through the fifth grade. Her family moved to High Point, NC before she started sixth grade. She attended Ferndale Middle School for sixth through eighth grades. She then attended High Point Central High School and graduated with honors in 1992. For college, she attended Campbell University in Buies Creek, NC for five semesters before transferring to North Carolina State University for a semester. She married her husband in July 1995 in Morganton, NC. She transferred to Appalachian State University in Boone, NC in the Fall 1995. She graduated form ASU with a B.S. in Chemistry (ACS certified degree) in 1997. She received a Master's in analytical chemistry from the University of Tennessee in Knoxville in 2004. She is currently staying at home raising her daughter, Caitlin, born in 2002.